Molecular dynamics simulations for electronic device design

FUJITSU LABORATORIES Ltd.
Chioko KANETA

Contents

1. Introduction:
Importance of high-throughput simulations in industry

2. Classical molecular dynamics simulations based on first-principles calculations
Oxidation process of Si/SiO_2 and SiC/SiO_2 interfaces

N. Takahashi, C. Kaneta (Fujitsu Labs.)
T. Yamasaki (Fujitsu Labs.->NIMS)
T. Ohno (NIMS, Univ. Tokyo)
S. Takamoto, S. Izumi, A. Hatano (Univ. Tokyo)
T. Kumagai (Central Research Institute of Electric Power Industry)

3. Design of Si/Ge structure with low thermal conductivity

N. Takahashi, C. Kaneta, Yu. Liu (Fujitsu Labs.)

Importance of high-throughput simulations in industry

Change of requirements for atomistic simulations

Means for understanding phenomena and mechanism→ Design tool

Obtain a hint or guideline to improve/design materials and their formation processes before starting developments within a short term

Screening:

a lots of simulations at once for variety of compositions

Materials informatics:

also requires a lot of simulations to search desirable materials

High throughput simulations such as classical molecular dynamics, tight bindng method etc.

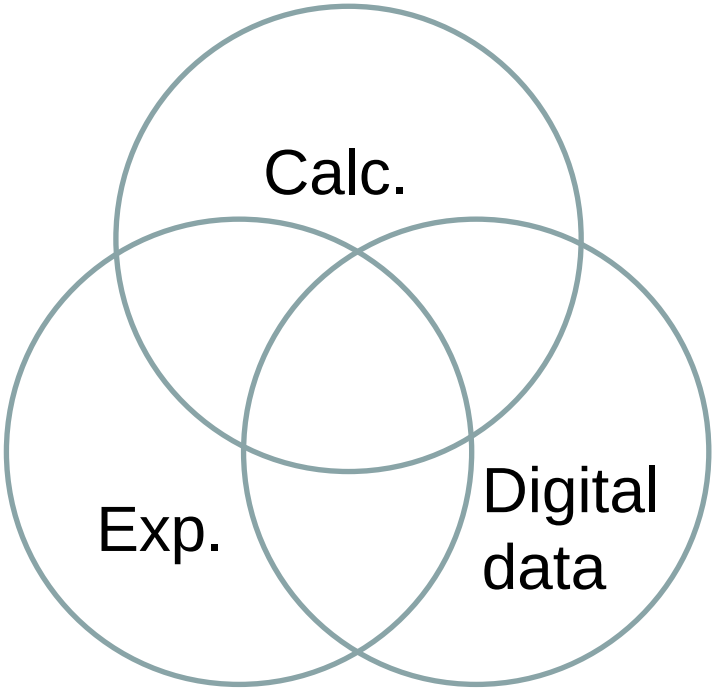

Why Si/SiO_2 interface?

Si/SiO_2 systems are used in various of semiconductor devices and also found in quantum dot solar cells, negative electrode of Li-ion rechargeable batteries etc.

Interface of Si/SiO_2

The most well-controlled, most important and most typical interface in industry, especially in semiconductor devices

There is a long history of the investigations of Si/SiO_2 interfaces, but they still attract great attention especially from the viewpoint of reliability.

- The mechanisms of degradation of gate dielectrics: Still controversial !
- Deal-Grove model
  → microscopic oxidation process of Si/SiO_2 interface

Reference of other semiconductor/oxide interfaces
SiC/SiO_2, GaN/Ga_2O_3, etc.

Importance of the Si/SiO_2 interface in MOSFET

MOS（Metal-Oxide-Semiconductor) Transistor

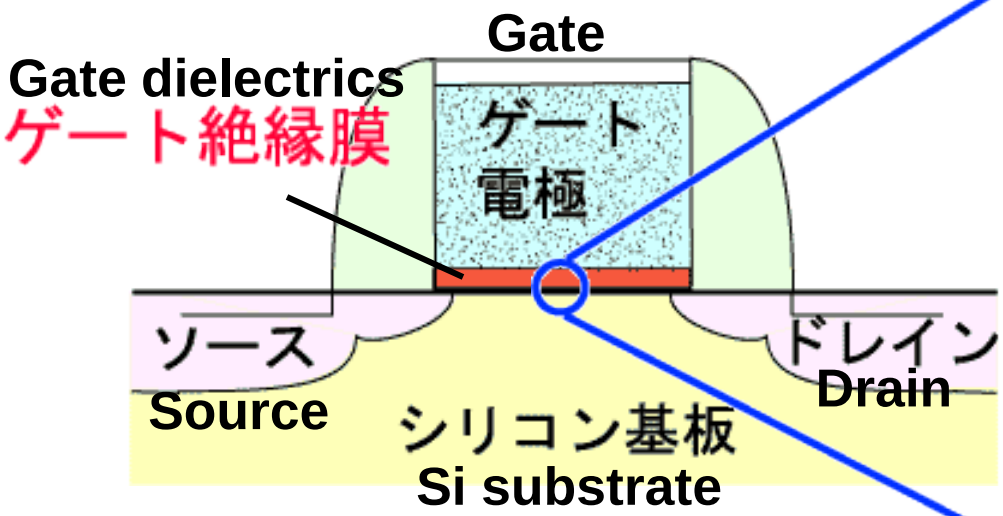

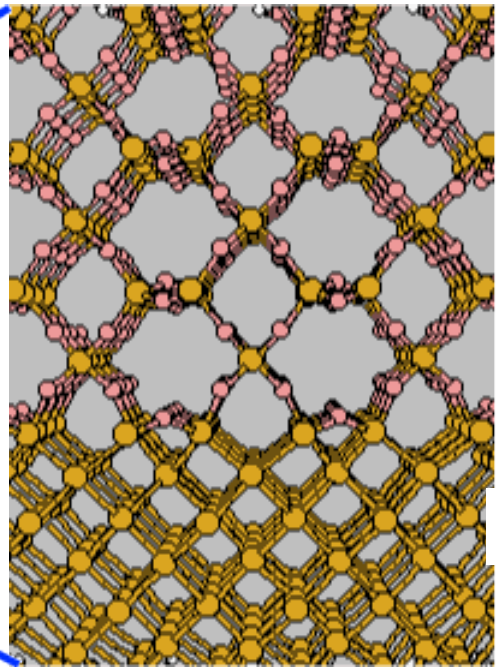

Active region of MOSFET

SiO_2 Gate dielectrics
about 1nm (3 - 4 SiO_2 layers）

↓

- **Increase of interfacial region**
- **Dielectric degradation by a few defects**

Downscaling of Si MOSFET

- Rapid downscaling of Si LSI → nano scale devices
- Novel materials and structures, importance of quantum effects → Quantum or atomistic simulation

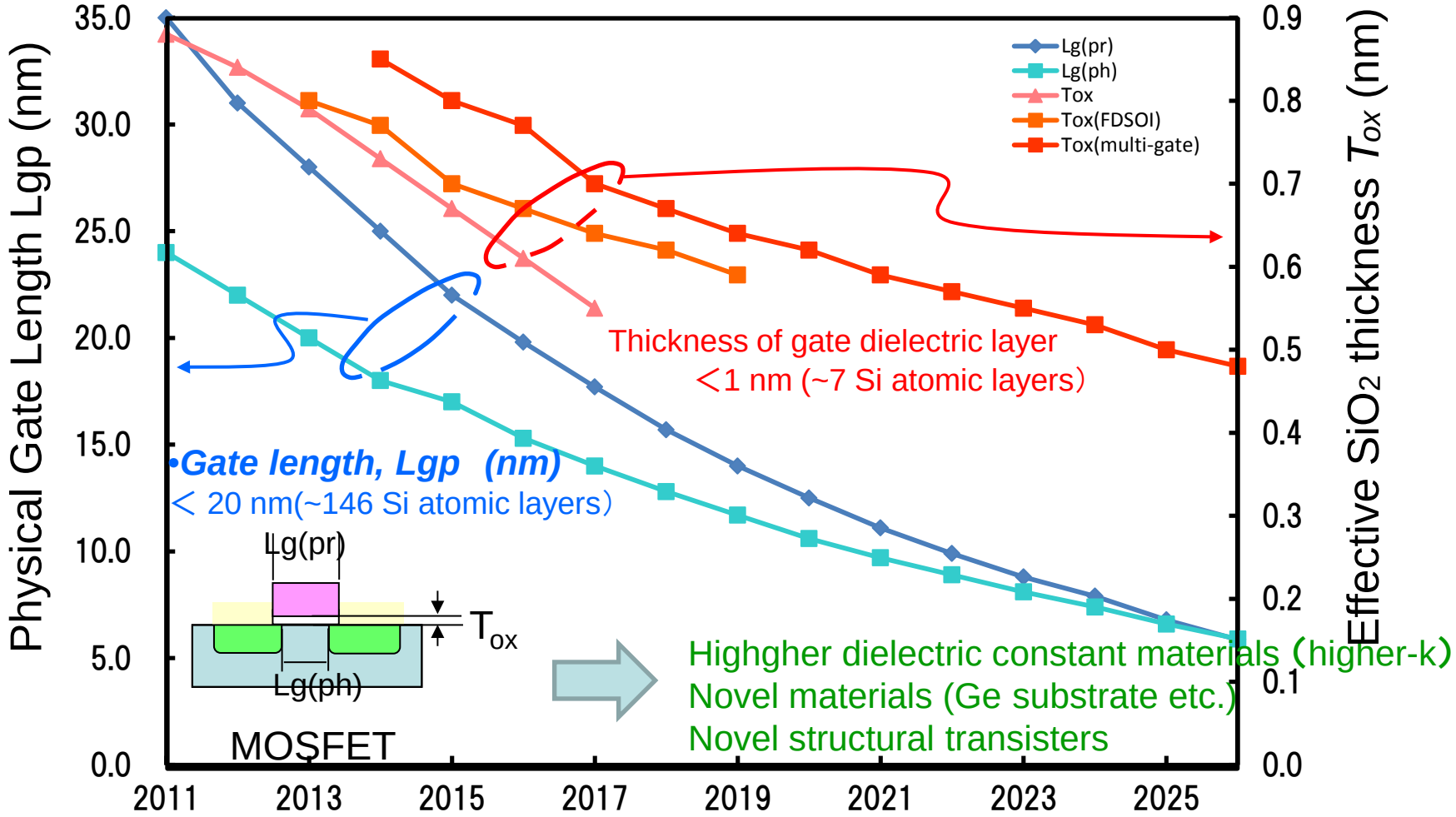

2012 International Semiconductor Roadmap (ITRS)HPD

How the electronic property changes at Si/SiO_2 interface？

Abrupt
No transition layer
Defect free

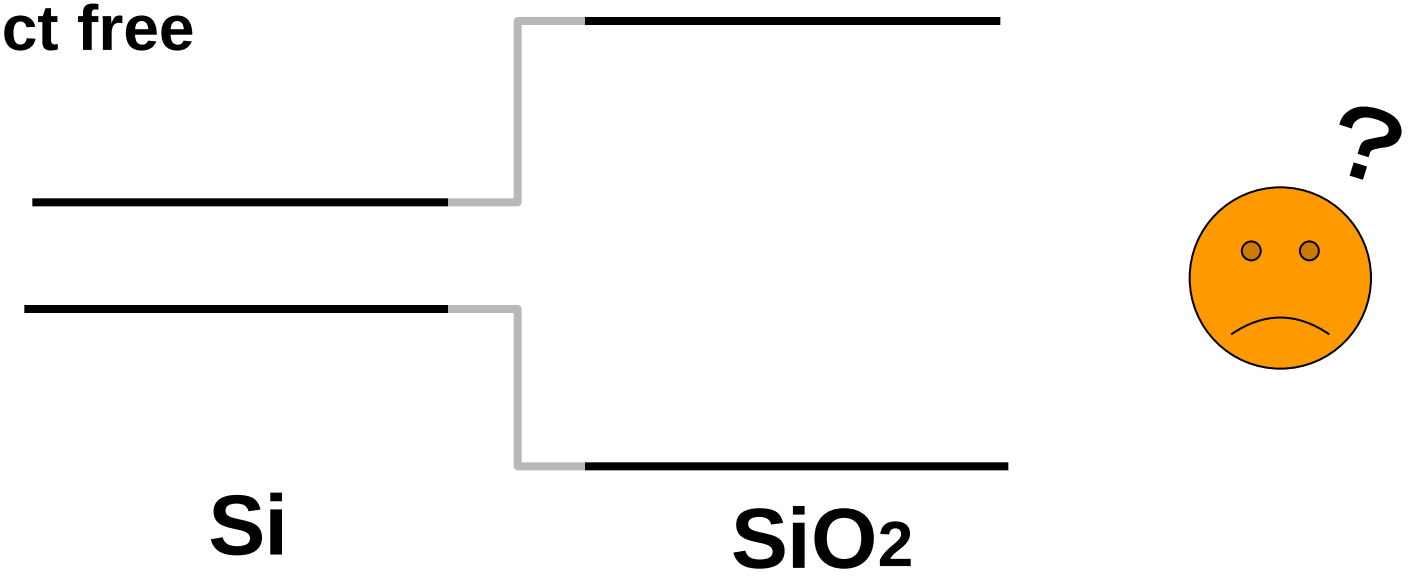

Different observation methods give different thicknesses of ultra-thin SiO_2 films.

Physical thickness＞ Optical thickness from ellipsometry
＞Electric thickness from capacitance measurement

Calculation method

First-principles method

DFT LDA + GGA

Pseudopotentials

Ultrasoft pseudopotential for O

D. Vanderbilt, Phys. Rev. **B41**, 7892 (1990)

Norm-conserving pseudopotential for Si and H

Troullier-Martins type : Phys. Rev. **B43**, 1993 (1991)

Periodic boundary condition **about 100 atoms/unit cell**

Cutoff energy

Charge dendity: 144Ryd.

Wave function 25Ryd.

4k-points

Three types of SiO_2 crystals are employed as initial structures of upper layer.

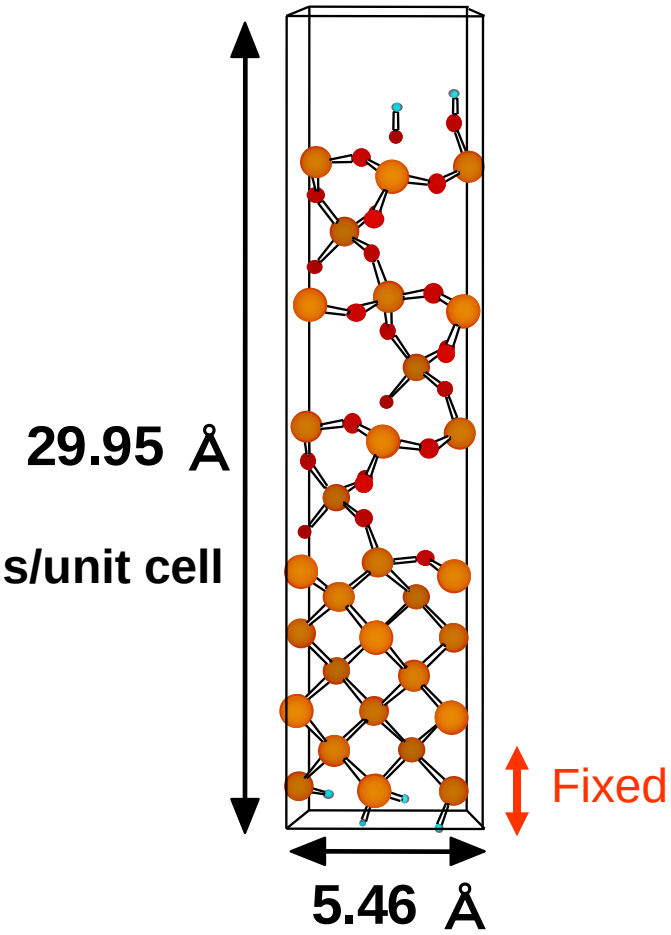

Unit Cell of Type-Q

Local DOS

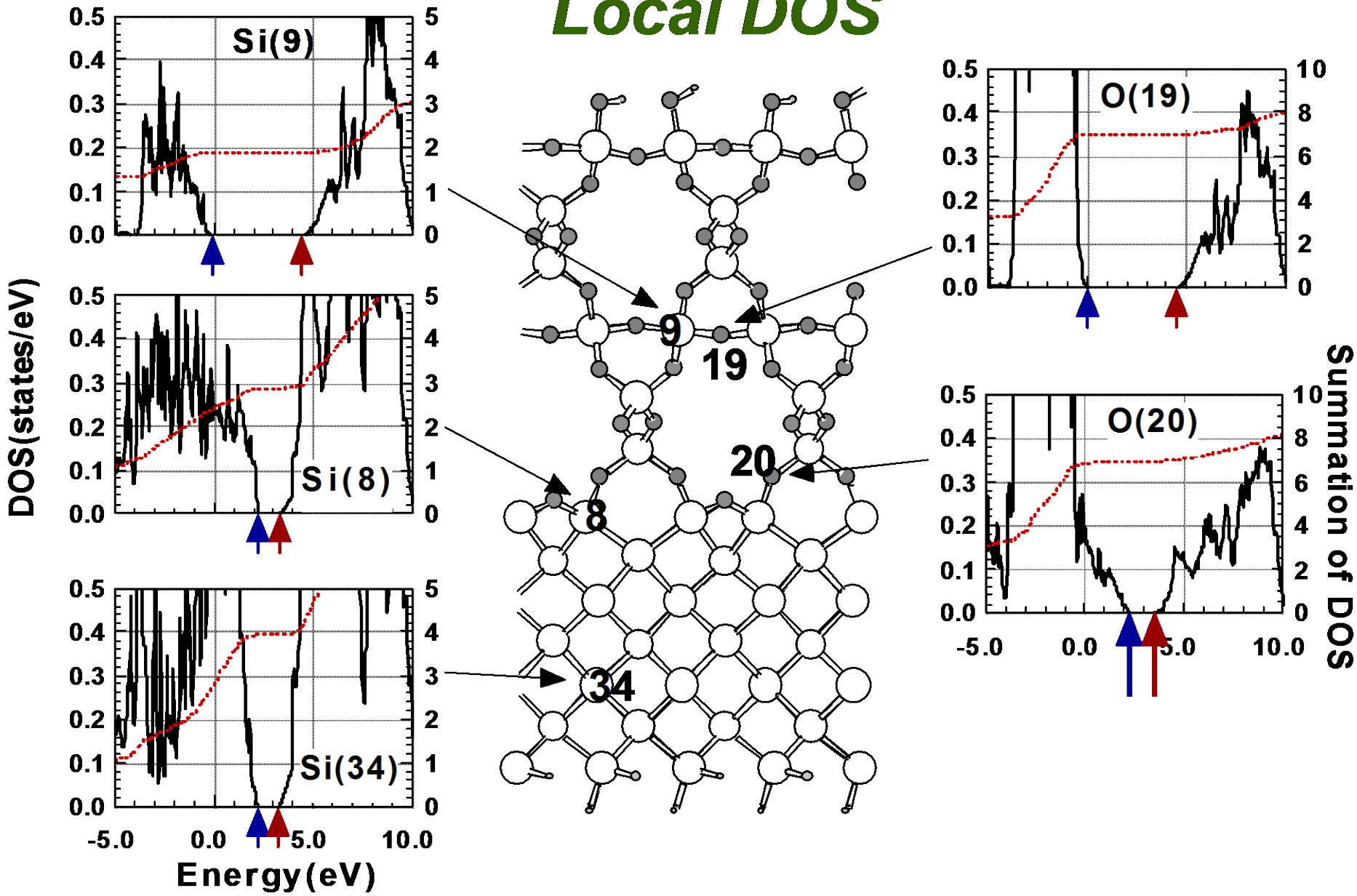
Si(9)
Si(8)
Si(34)
O(19)
O(20)
DOS(states/eV)
Summation of DOS
Energy(eV)
9
19
20
8
34

Energy band variation at Si/SiO2 interface

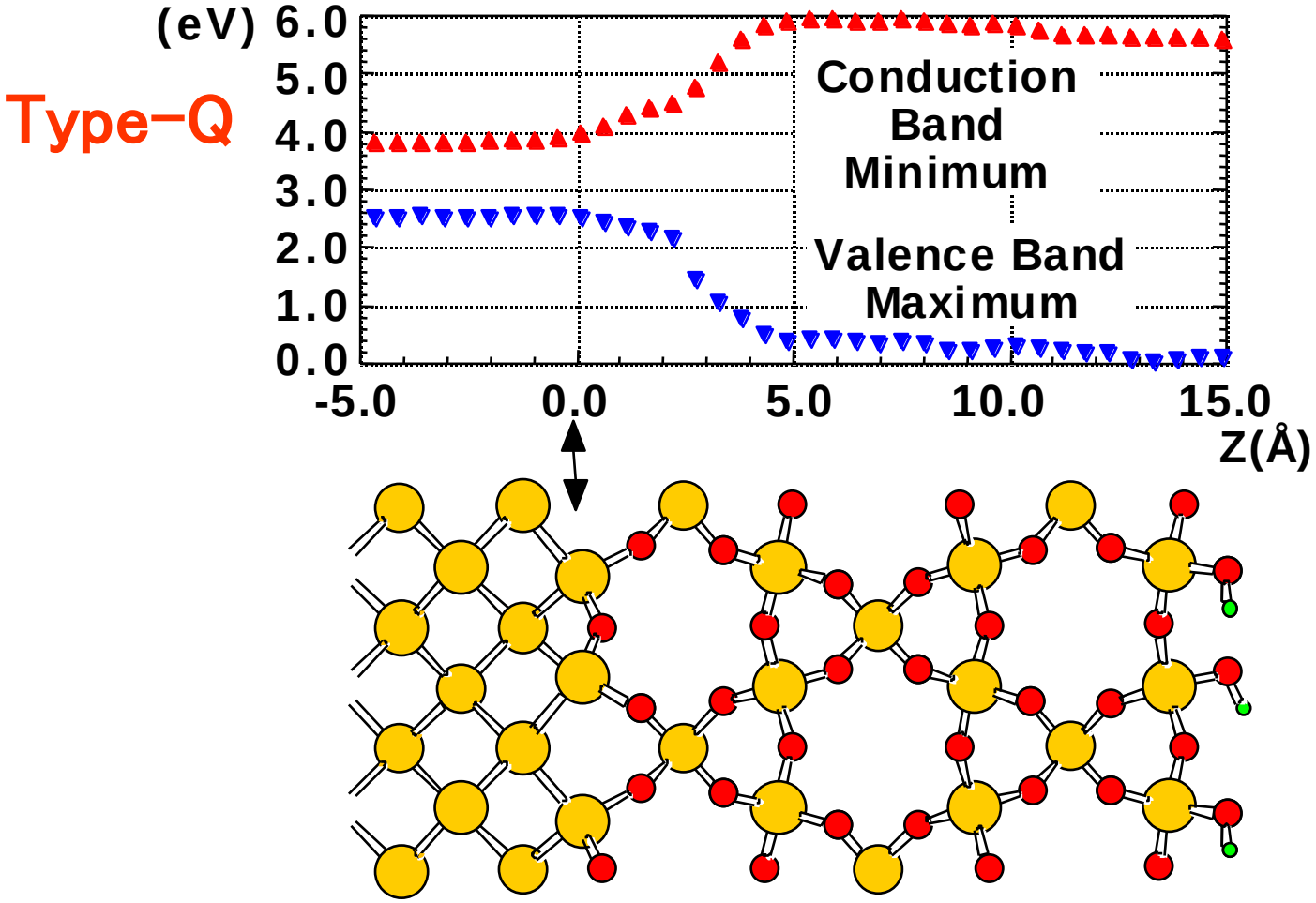

Kaneta et al. Microelectronic Engineering **48**, 117 (1999)

Yamasaki et al. Phys. Rev. B 63, 115314 (2001)

Oxidation of Si

There are a great deal of research,
but no pictures on the dynamics of emissions and incorporation of Si species in a particular microscopic framework.

- Oxidation processes
- Formation of interface structures
- Defect formation in the oxides, substrates, and interfaces

→*Hints for production processes design*

Atomistic model of silicon oxidation processes

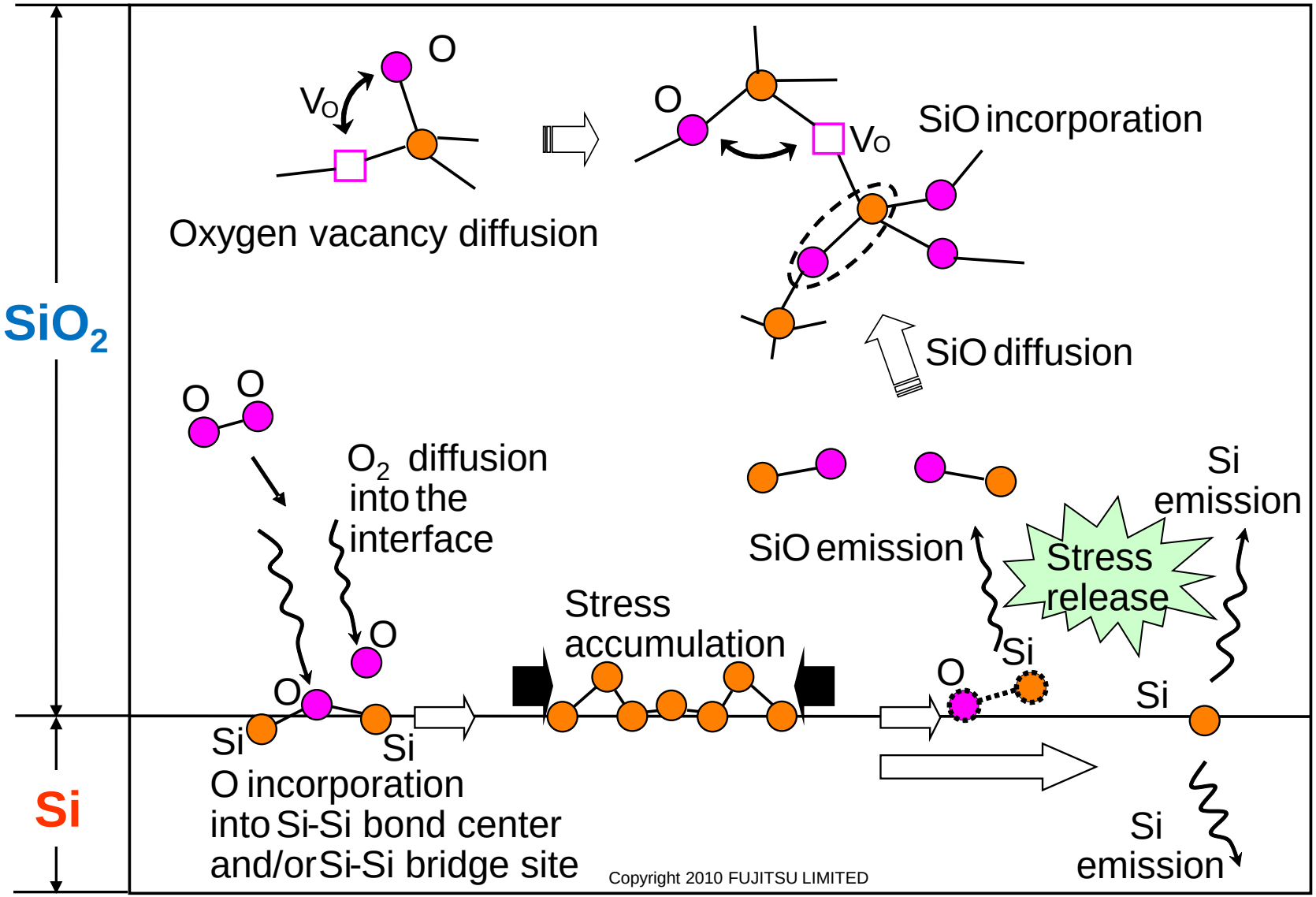

Copyright 2010 FUJITSU LIMITED

Effective atomic charges in Si/SiO_2

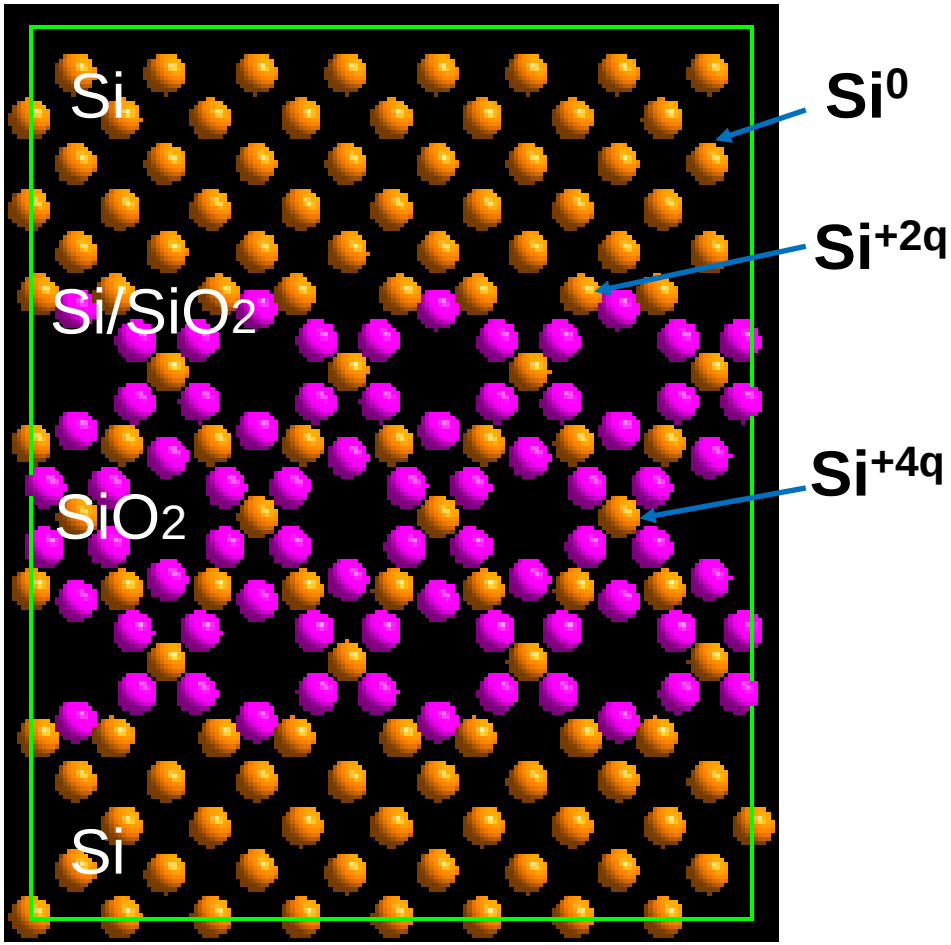

Effective atomic charge should be defined depending on the configuration.

Extended Tersoff type interatomic potentials for classical molecular dynamics

Variable charge on each atom is determined in the framework of the charge equilibration method

$$
\begin{aligned}
\Phi &= \sum_i E_i^{self} + \frac{1}{2}\sum_{i\neq j}\phi_{ij} \\
\phi_{ij} &= E_{ij}^{rep} + E_{ij}^{cov} + E_{ij}^{ion} \\
E_i^{self} &= E_i^0 + \underline{\chi q_i} + \frac{1}{2}Jq_i^2 \\
E_{ij}^{rep} &= f_c(r_{ij})\left(1+\frac{Q}{r_{ij}}\right)A\exp(-\lambda_A r_{ij}) \\
E_{ij}^{cov} &= f_c(r_{ij})\,f_q(q_i)\,b_{ij}\sum_{m=1,3}B_m\exp(-\lambda_{B_m}r_{ij}) \\
E_{ij}^{ion} &= \frac{q_i q_j}{r_{ij}} \\
b_{ij} &= \left(1+\zeta_{ij}^{\eta}\right)^{-\delta} \\
\zeta_{ij} &= \sum_{k\neq i,j} f_c(r_{ik})\left\{c+d\left(h-cos\theta_{ijk}\right)^2\right\} \\
&\times \exp\left[\alpha\left\{\left(r_{ij}-R_{ij}^e\right)-\left(r_{ik}-R_{ik}^e\right)\right\}^{\beta}\right] \\
f_c(r_{ij}) &= \begin{cases} 1 & r_{ij}\leq R_1 \\ \frac{1}{2}\left[1+cos\left(\frac{\pi(r_{ij}-R_1)}{R_2-R_1}\right)\right] & R_1<r_{ij}<R_2 \\ 0 & r_{ij}\geq R_2 \end{cases} \\
f_q(q_i) &= \frac{N_i(q_i)\left(N_i^0-N_i(q_i)\right)}{N_i(0)\left(N_i^0-N_i(0)\right)} \\
N_i(q_i) &= N_i^{neutral} - q_i
\end{aligned}
$$

[1] A. K. Rappé and W. A. Goddard III, J. Phys. Chem. 95, 3358 (1991).

[2] T. Kumagai, S. Izumi. S. Hara, S. Sakai, ICCM 2004, Singapore, 2004, Conference Digest pp. 75.

Description of the effective force field for classical MD simulations

The parameters are obtained by fitting to data, which are gathered from experimental and/or from quantum chemical calculations.

Within the harmonic description of the bond length/bond energy relationship, it is impossible to describe the dissociation,

Parameters determined with large amount of values from first-principles calculations on many kinds of reference systems.

[Ref.] T. Kumagai et. al, ICCM 2004, Singapore, 2004, Conference Digest pp. 75.

van Duin et al. J. Phys. Chem. A 107, 3803 (2003).

Variable charge method

Concept

Atomic charges are determined to minimize total electrostatic energy *E* in each configuration.

A. K. Rappé et al., J. Phys. Chem. 95, 3358 (1991).

- Atomic chemical potentials ($\chi_i \equiv \partial E / \partial Q_i$) are equal :

$$\chi_1 = \chi_2 = \cdots = \chi_N \qquad (1)$$

- Total charge is constant :

$$Q_{\mathrm{tot}} = \sum_{i=1}^{N} Q_i \qquad (2)$$

Solving a total of *N* simultaneous equations of charges Q_i (QEq equations) gives an optimal set of $\{Q_1, Q_2, \ldots, Q_N\}$.

Diatomic Coulomb integrals between all pairs of atoms are evaluated employing Slater-type 1s functions with originally optimized Slater exponents to involve screening correction.

Flow and conditions of classical molecular dynamics simulations

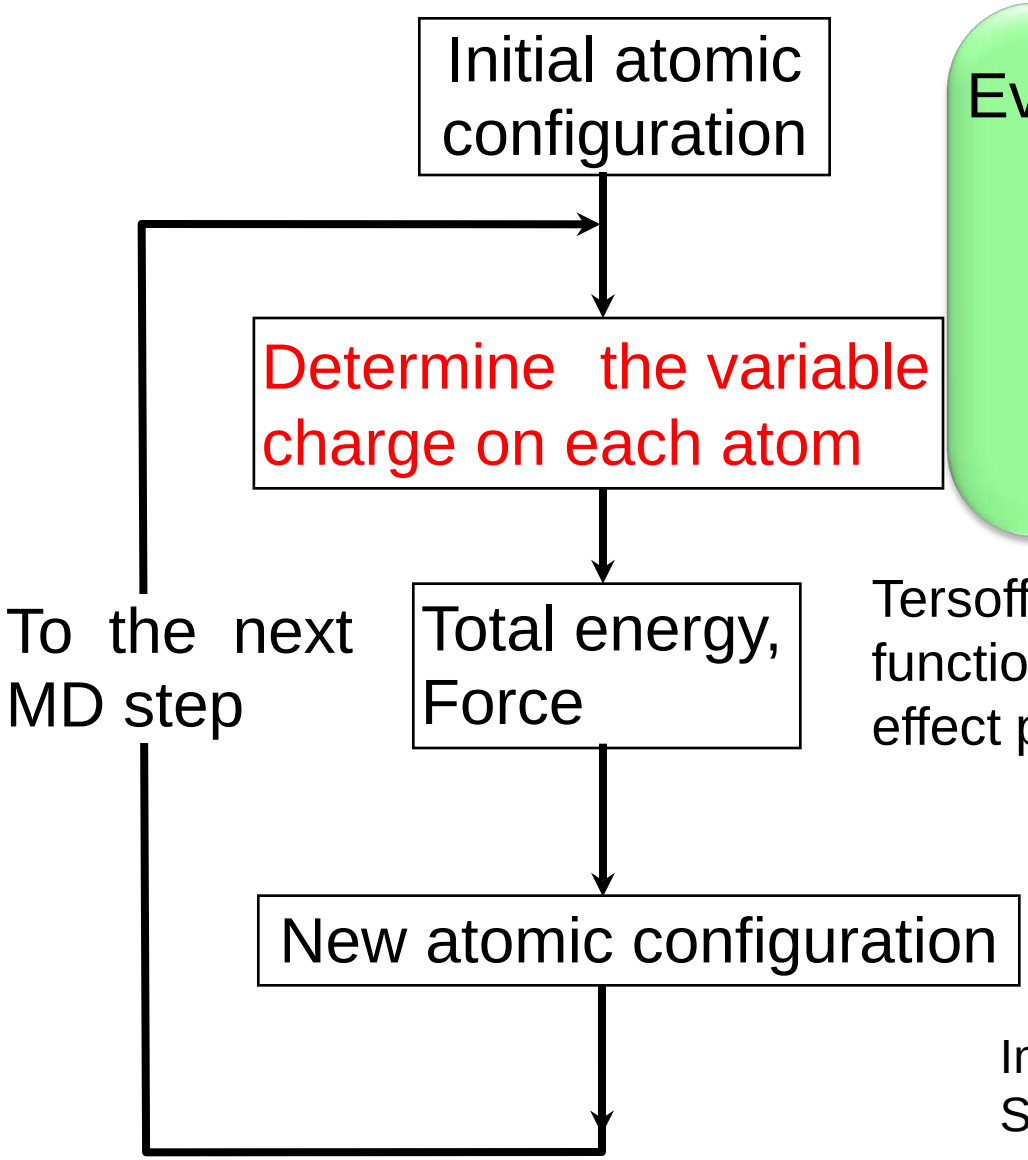

Evaluation of energy barriers

NTP ensembles

100ps ×10-20 MD trials

with different velocity distributions

→1-2 ns

comparable with the time of elementary process to occur

Tersoff type three-body potential functions[1] with the charge transfer effect parameterized by Kumagai et al.[2]

1) J. Tersoff, Phys. Rev. Lett. **56**, 632 (1986); Phys. Rev. **B 39(8)**, 5566 (1989).

2) T. Kumagai et al., ICCM 2004, Conference Digest pp. 75.

Implemented to the MD program SCIGRESS MD-ME (FUJITSU)

Lattice constant, density, and bond length of Si, SiO_2

Lattice constant

		this work (Å)	exp. (Å)	Δ (%)
Si		5.44	5.43	+0.2
SiO_2	a,b	4.89	4.91	-0.4
	c	5.37	5.40	-0.6

Density

	this work (g/cm^3)	exp. (g/cm^3)	Δ (%)
Si	2.32	2.33	-0.4
SiO_2	2.68	2.64	+1.5

Radial distribution function @ 298K

Si-Si in c-Si

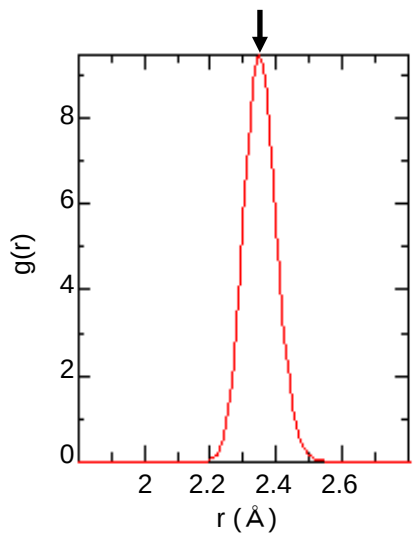

Si-O in c-SiO_2

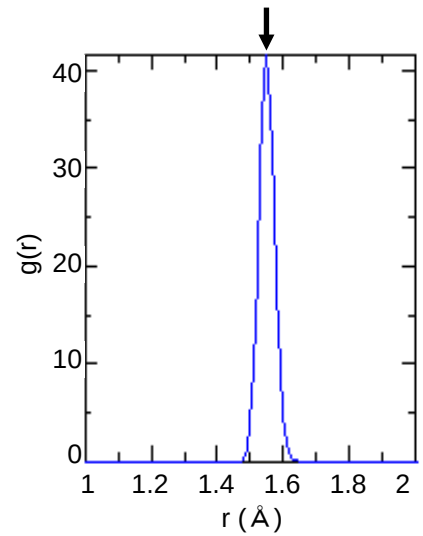

c-Si

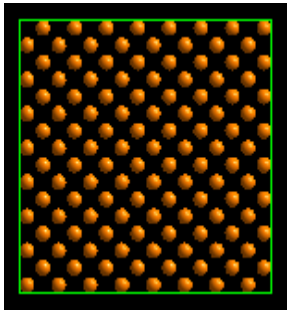

α-quartz

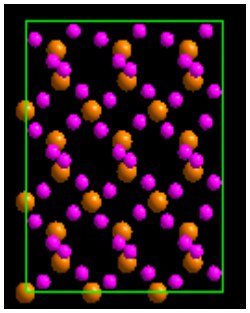

Change of atomic charges at the Si/SiO_2 interface

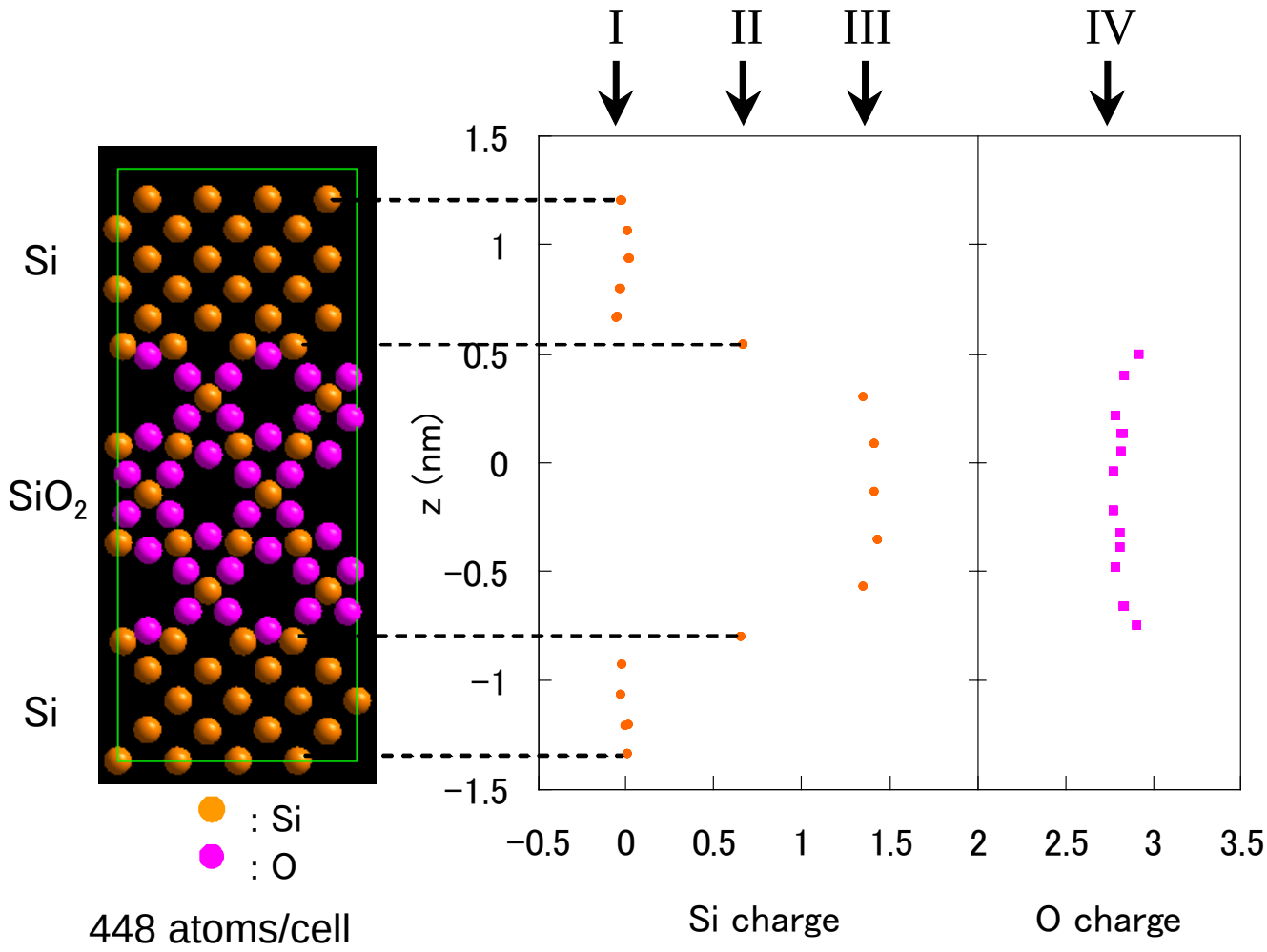

Figure 1. Si/SiO_2 structure and charges of Si and O atoms.

Takahashi et al. Mol. Sci. 2, NP010 (2007),
5th Int. Symp. On Controt of Semiconductor Interfaces(2007)

Initial structure of Si(100)/SiO_2 interface

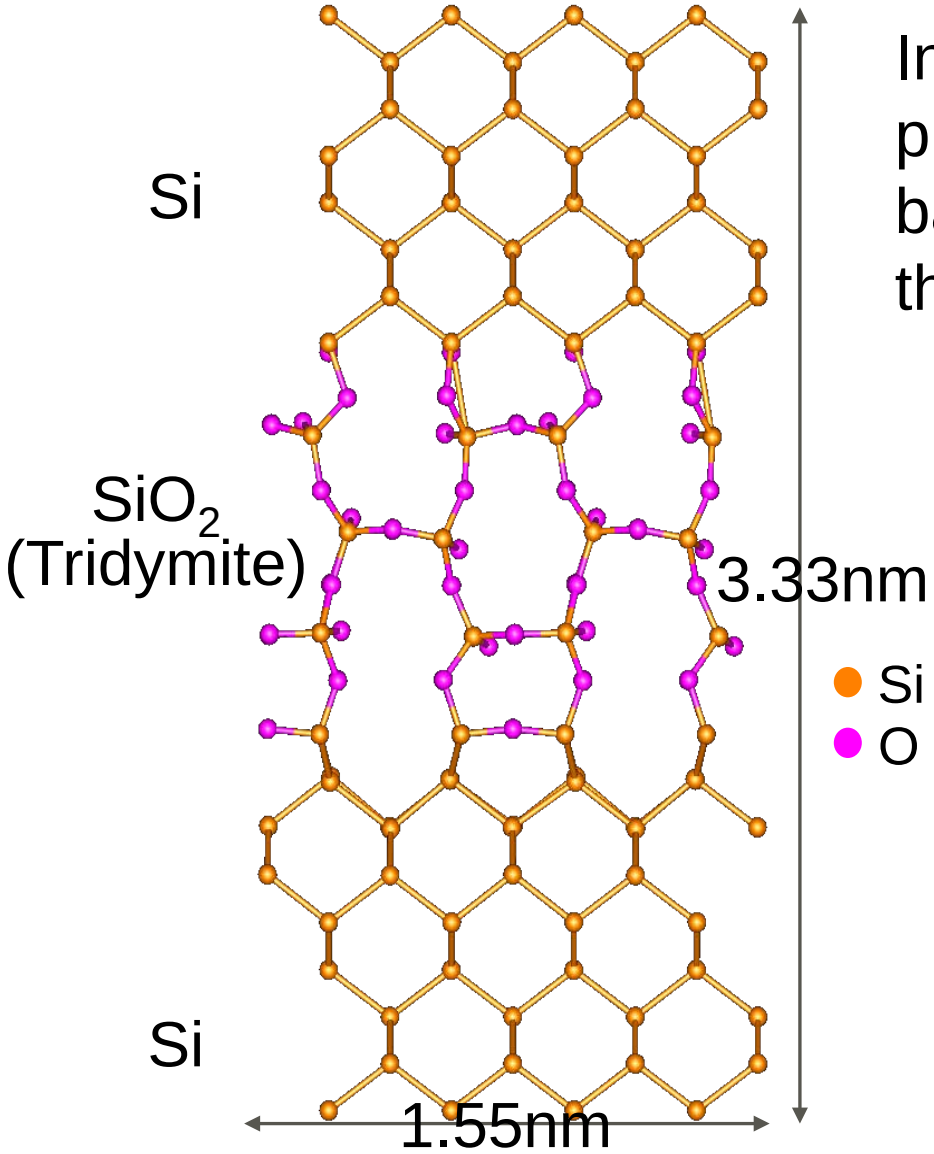

Initial Si(100)/SiO_2 structure prepared for MD simulation based on the result of the first-principles calculations[1,2)]

- 3D periodic boundary condition
- 448 atoms in the unit cell

1) C. Kaneta et al., Microelectronic Engineering **48**, 117 (1999);
2) T. Yamasaki et al., Phys. Rev. B **63**, 115314 (2001).

Si/SiO_2 model with interfacial stress by excess O atoms

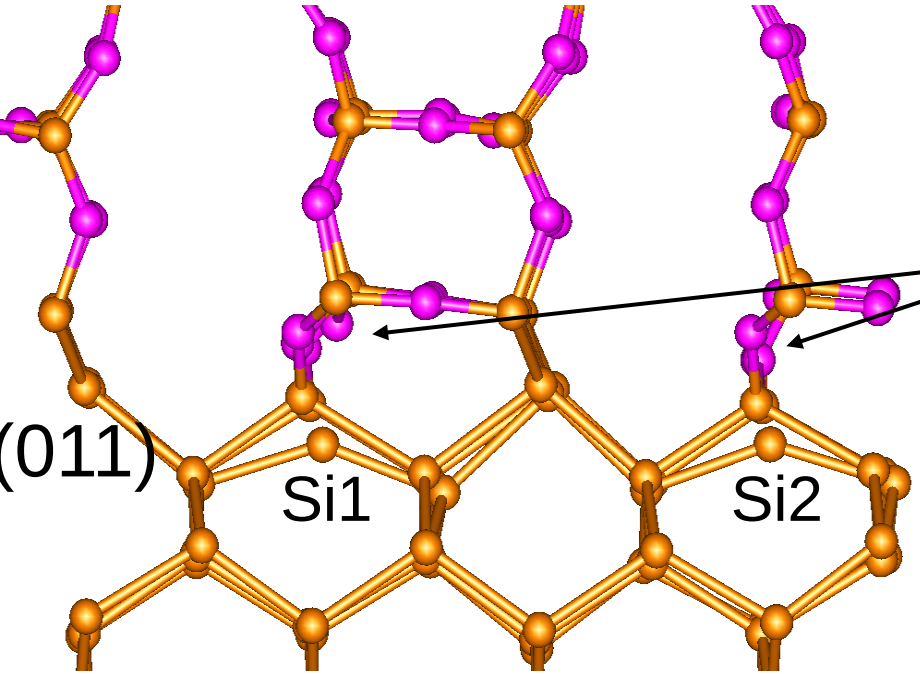

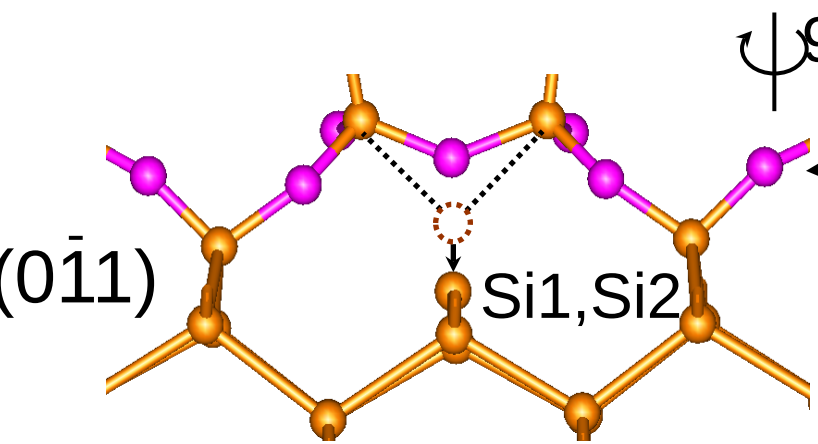

10 O atoms are introduced into the Si-Si bond center and Si-Si bridging sites at the interface.

MD simulations for structural relaxation

constant NTP conditions

N=458, T=25℃, P=1atm

2-folded Si (Si1 and Si2) are formed and behave as the reactive sites in the following oxidation steps.

Si emission into the Si substrate

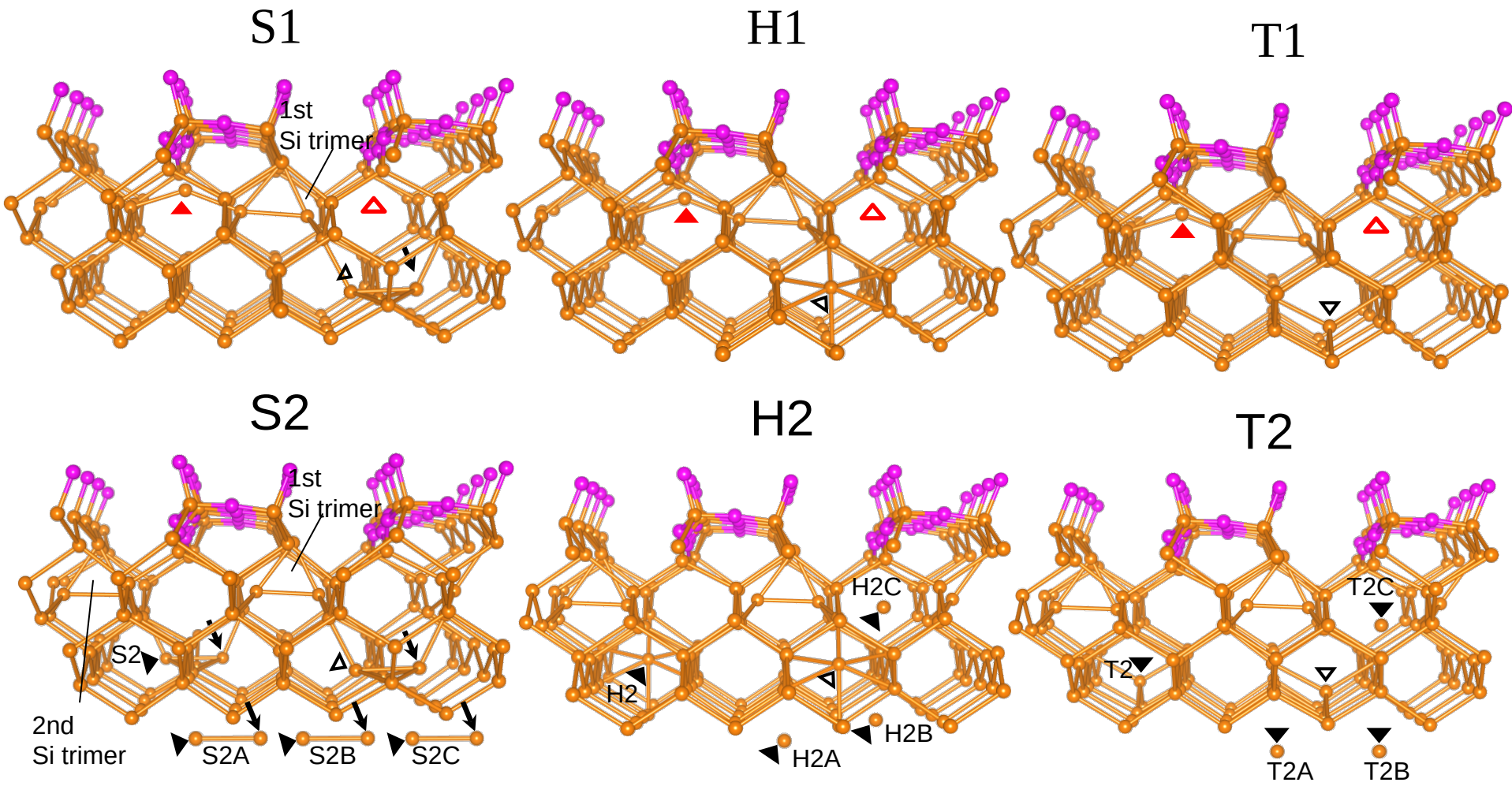

Split-110 Hexagonal site Tetrahedral site

Si emission into the SiO_2 region

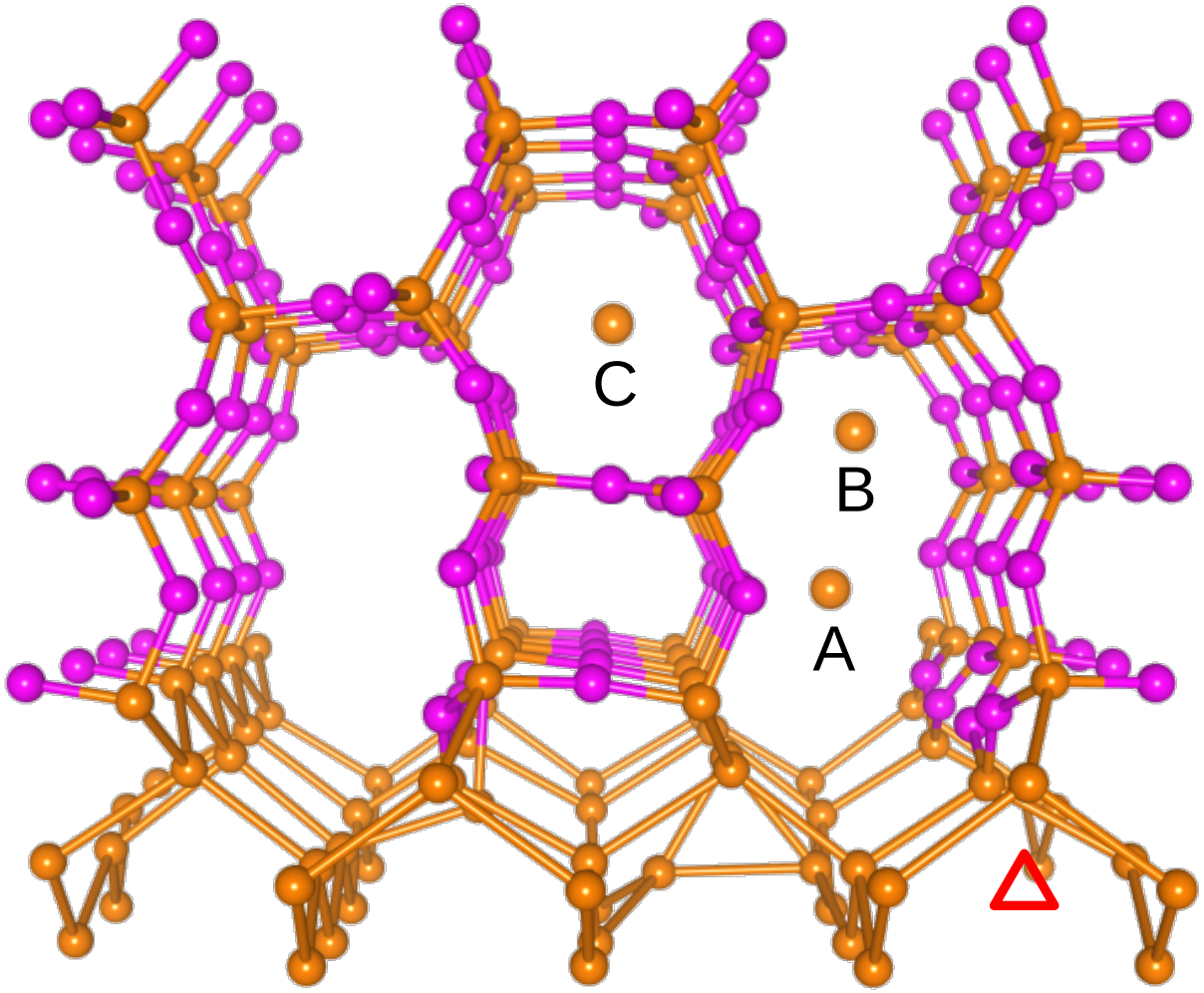

Possible sites for Si interstitials in SiO_2

O atoms in the vicinity of 2-folded Si

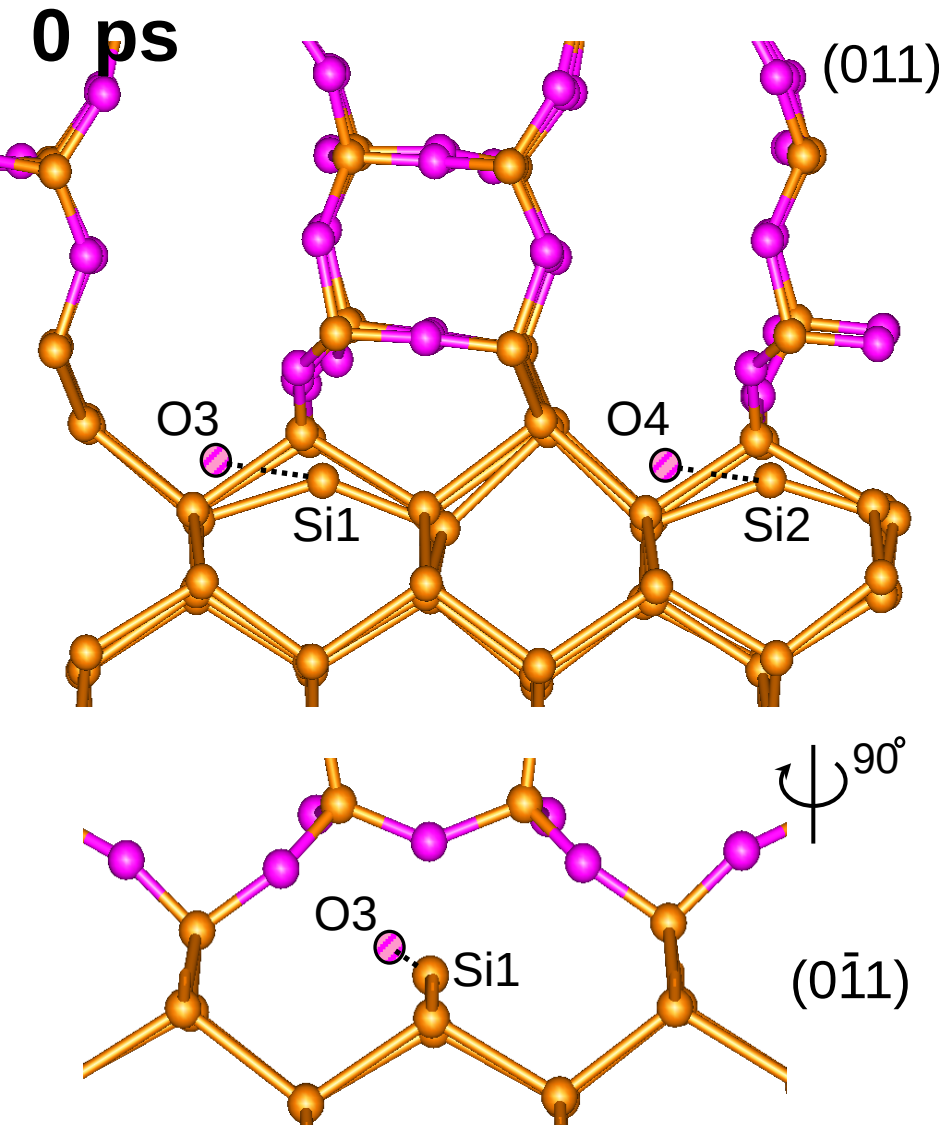

Two other O atoms (O3 and O4) are introduced in the vicinity of 2-folded Si.

MD simulation

constant NTP conditions, N=460, T=1400℃, P=1atm

SiO emission at the Si/SiO_2 interface

31 ps

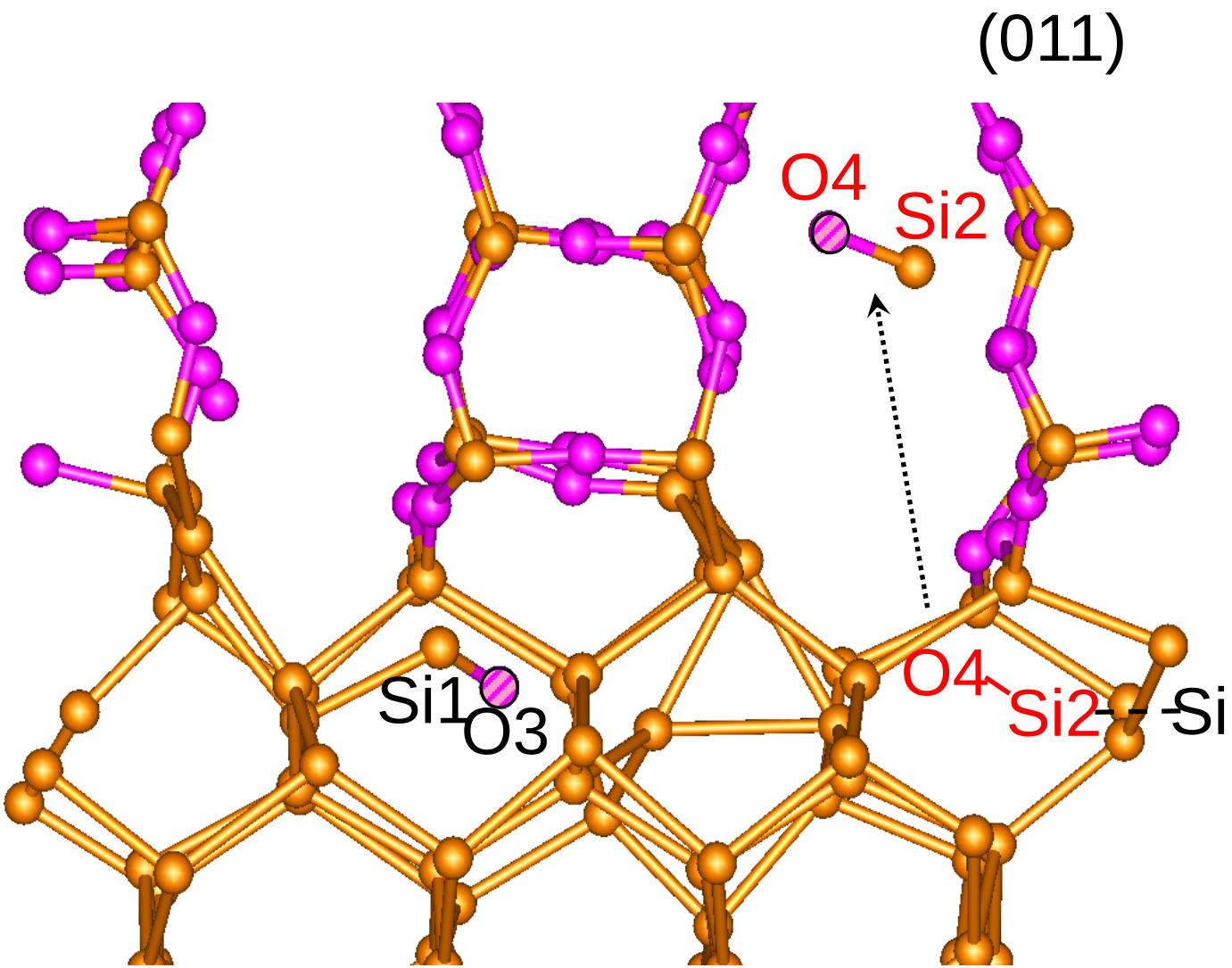

1) N. Takahashi, T. Yamasaki, and C. Kaneta, J. Appl. Phys. 115, 224303 (2014).

2) N. Takahashi, T. Yamasaki, and C. Kaneta, Phys. Status Solidi B 251, pp.2169-2178(2014). (*Invited*)

Change of enthalpy in SiO emission

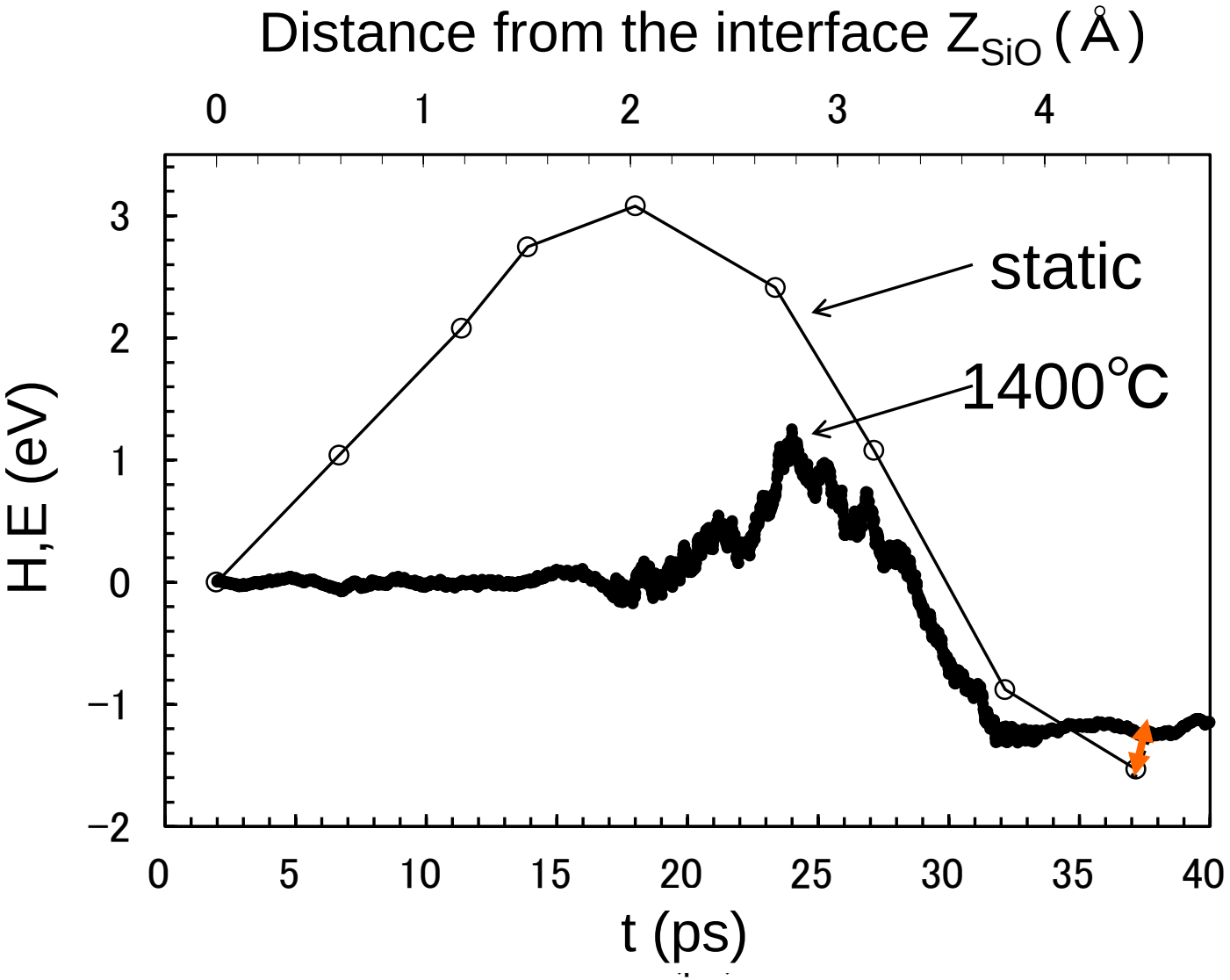

ΔHdynamical=1.2eV
ΔEstatic=3.08eV
ΔEfp=2.81eV

1) N. Takahashi, T. Yamasaki, and C. Kaneta, J. Appl. Phys. 115, 224303 (2014).

2) N. Takahashi, T. Yamasaki, and C. Kaneta, Phys. Status Solidi B 251, pp.2169-2178(2014). (*Invited*)

SiO and O-vacancy in SiO_2

a-SiO_2

● Si
● O

SiO at an interstitial site in SiO_2

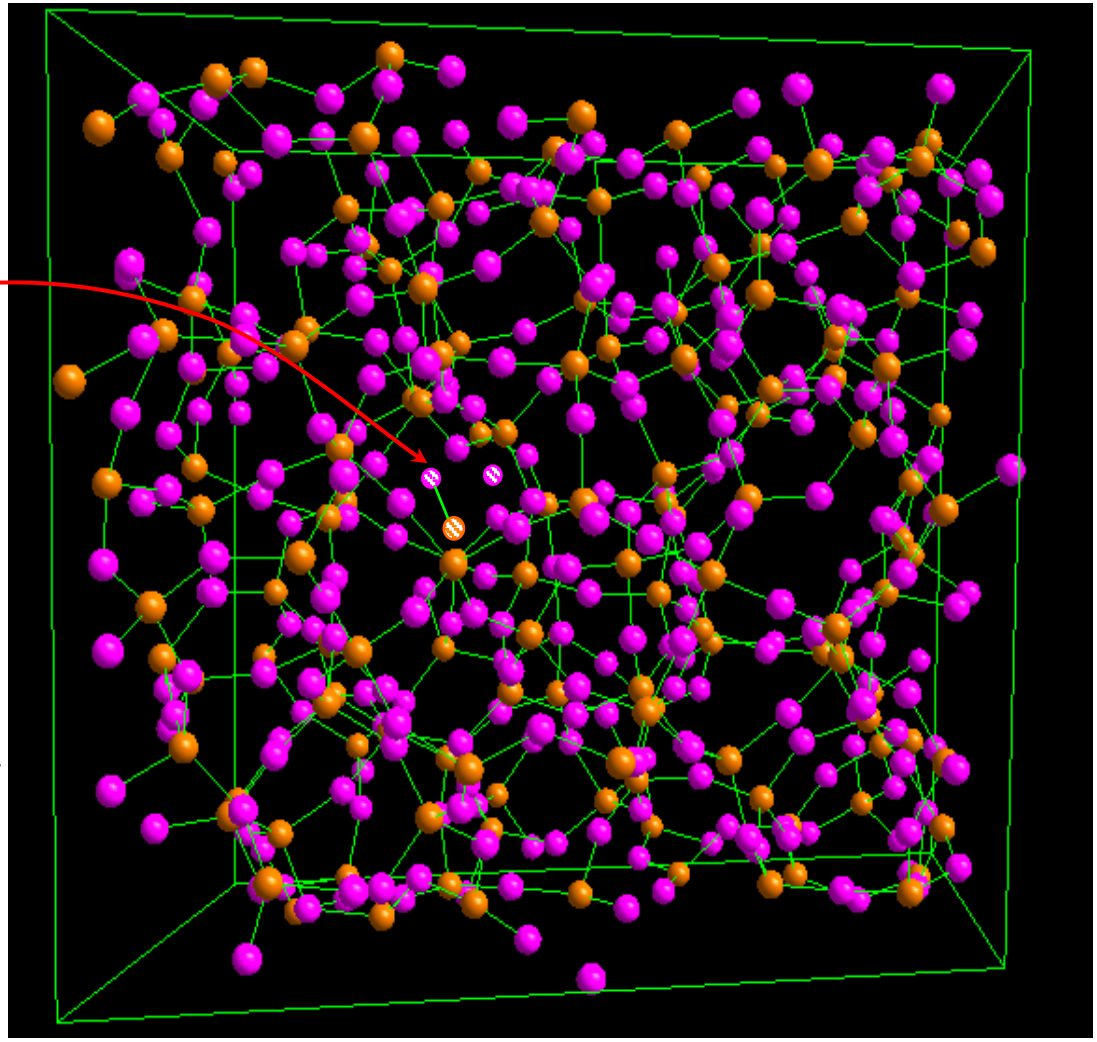

- 435 atoms in unit cell
- Periodic boundary condition
- constant NTP
- T = 1400℃

Takahashi et al. Proc. of the 217th Electrochemical Society Meeting 2010. ECS Transactions, 28(1) 361-368 (2010) 10.1149/1.3375622.

Change of enthalpy in SiO incorporation into SiO_2

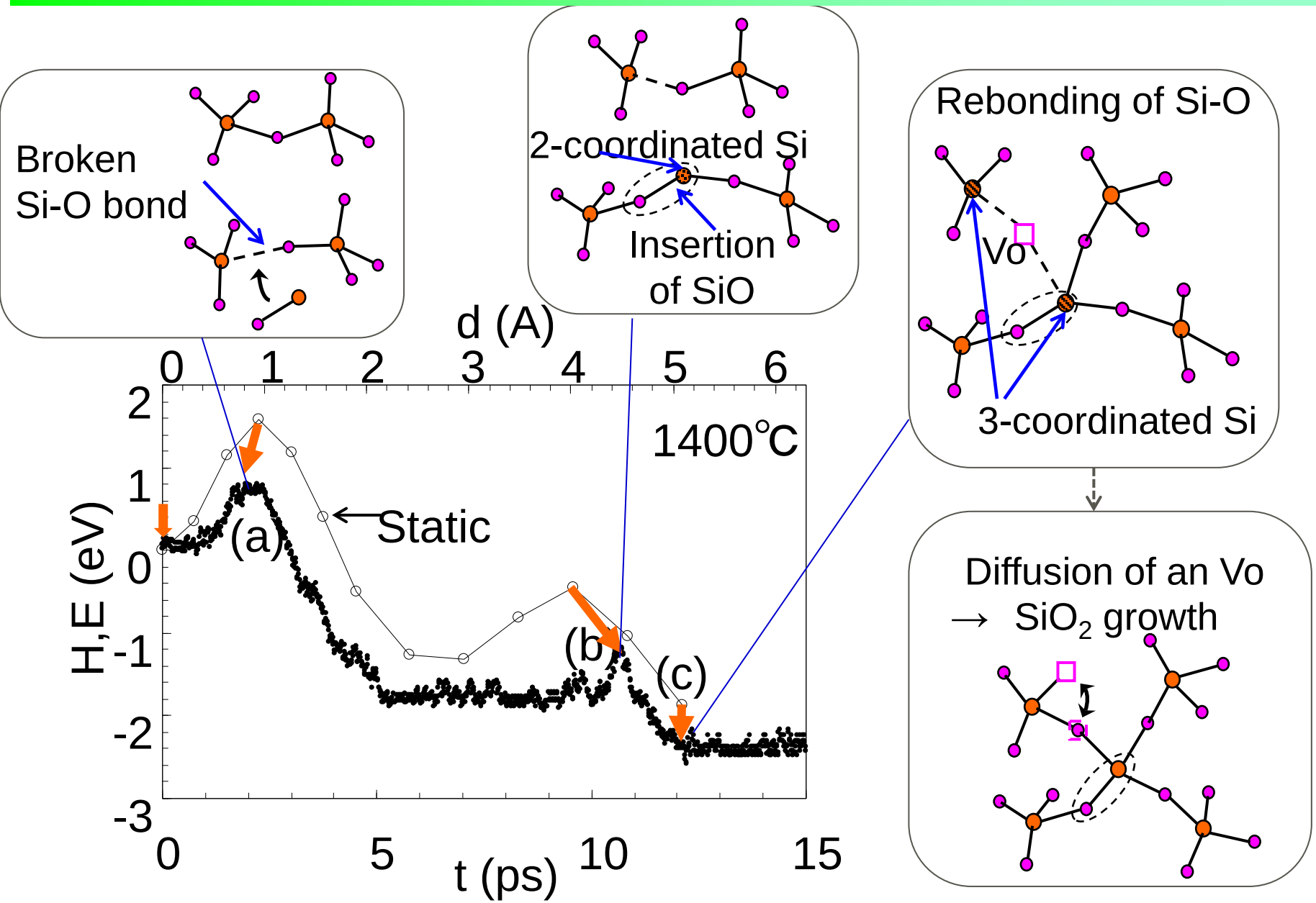

1) N. Takahashi, T. Yamasaki, and C. Kaneta, J. Appl. Phys. 115, 224303 (2014).

2) N. Takahashi, T. Yamasaki, and C. Kaneta, Phys. Status Solidi B 251, pp.2169-2178(2014). (*Invited*)

Energy gain in the oxidation processes with SiO emission

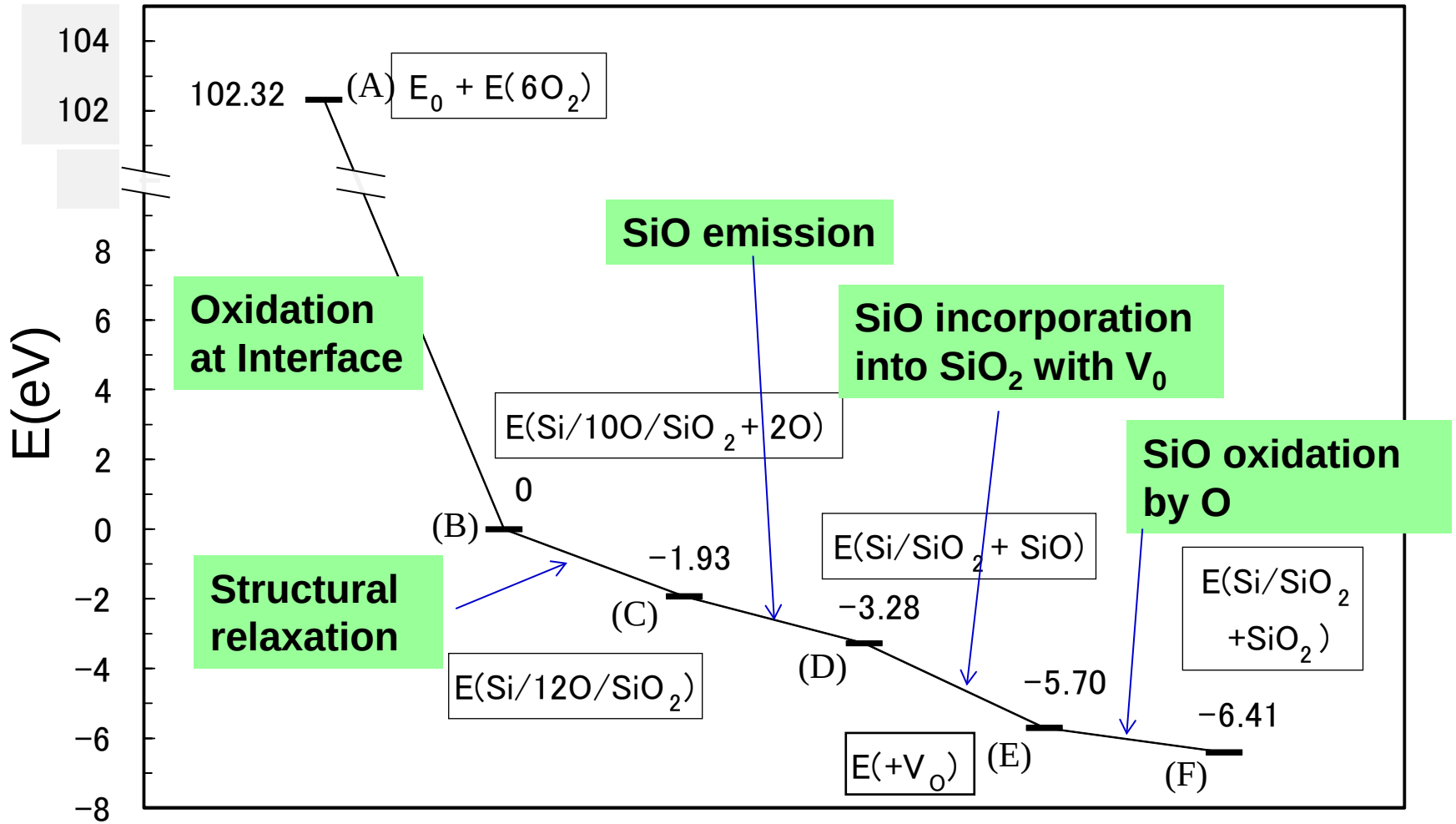

1) N. Takahashi, T. Yamasaki, and C. Kaneta, J. Appl. Phys. 115, 224303 (2014).

2) N. Takahashi, T. Yamasaki, and C. Kaneta, Phys. Status Solidi B 251, pp.2169-2178(2014). (*Invited*)

ReaxFF energy terms

$$E_{system} = E_{bond} + E_{lp} + E_{over} + E_{under} + E_{val} + E_{pen} + E_{coa} + E_{C2} + E_{tors} + E_{conj} + E_{H-bond} + E_{vdWaals} + E_{Coulomb}$$

- E_{bond}: bond energy; attractive term, directly derived from bond orders
- E_{lp}: Lone pair energy; penalty for breaking up lone pairs in O, N
- E_{over}: Overcoordination energy: penalty for overcoordinating atoms
- E_{under}: Undercoordination energy: stabilizes undercoordinated atoms
- E_{val}: Angle strain; equilibrium angle depends on bond order central atom
- E_{pen}: Penalty for 'allene'-type molecules ($H_2C=C=CH_2$)
- E_{coa}: Angle conjugation; stabilizes $-NO_2$ groups
- E_{C2}: C_2 correction: destabilizes C=C
- E_{tors}: Torsion energy: bond-order dependent V_2-term
- E_{conj}: Torsion conjugation: general conjugation stability
- $E_{H\text{-}bond}$: Hydrogen bond
- $E_{vdWaals}$: van der Waals: calculated between every atom
- $E_{Coulomb}$: Coulomb interaction: calculated between every atom; polarizable charges get updated every iteration

General

Special case

van Duin et al. J. Phys. Chem. A 107, 3803 (2003).

Force Field Parameters

van Duin et al. J. Phys. Chem. A 107, 3803 (2003).

Parameters are obtained by *ab initio* calculatios.

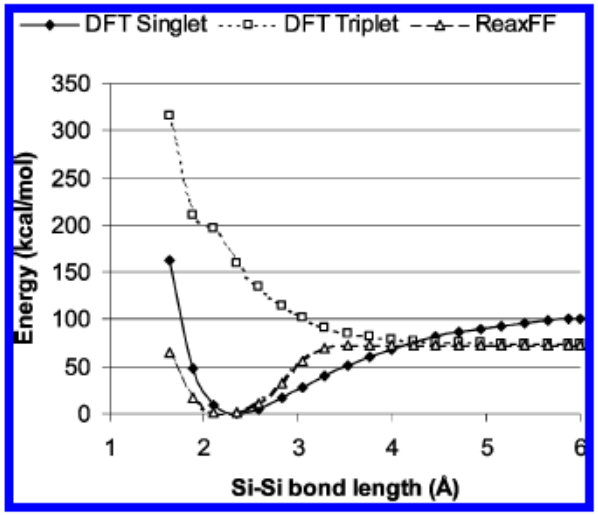

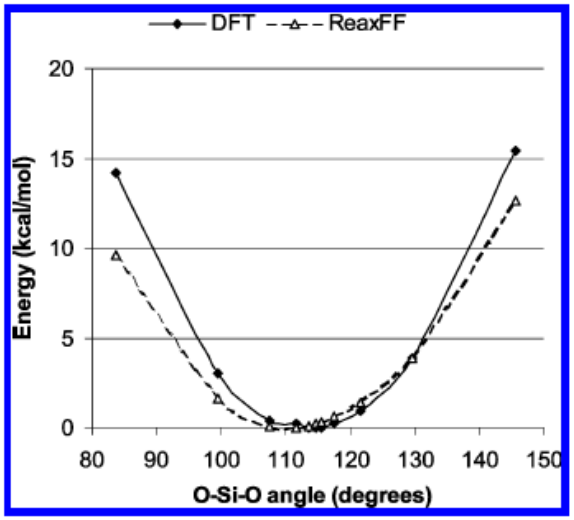

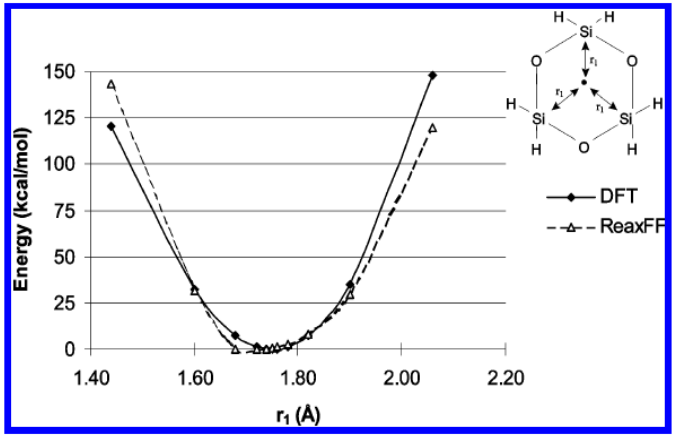

Figure 10. Distortion energies for c-$(SiH_2O)_3$ ring for DFT and $ReaxFF_{SiO}$.

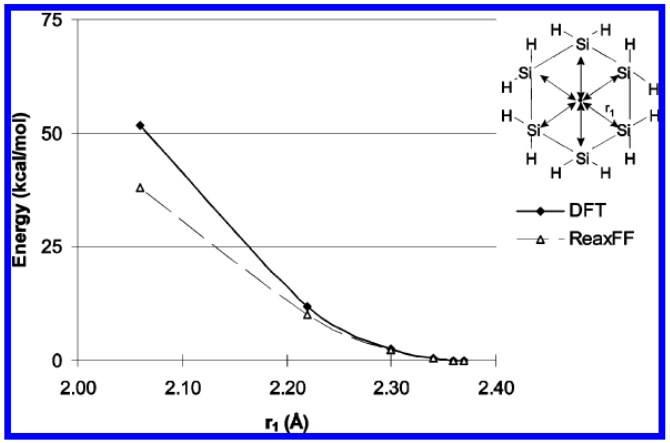

Figure 11. Distortion energies for c-$(SiH_2)_6$ ring for DFT and $ReaxFF_{SiO}$.

ab initio calculations are performed on hundreds of molecules.

Atomic charges depend on the atomic configurations.

Extended Tersoff type interatomic potentials for classical molecular dynamics

Variable charge on each atom is determined in the framework of the charge equilibration method

$$
\begin{aligned}
\Phi &= \sum_i E_i^{self} + \frac{1}{2}\sum_{i\neq j}\phi_{ij} \\
\phi_{ij} &= E_{ij}^{rep} + E_{ij}^{cov} + E_{ij}^{ion} \\
E_i^{self} &= E_i^0 + \underline{\chi q_i} + \frac{1}{2}Jq_i^2 \\
E_{ij}^{rep} &= f_c(r_{ij})\left(1+\frac{Q}{r_{ij}}\right)A\exp(-\lambda_A r_{ij}) \\
E_{ij}^{cov} &= f_c(r_{ij})\, f_q(q_i)\, b_{ij} \sum_{m=1,3} B_m \exp(-\lambda_{B_m} r_{ij}) \\
E_{ij}^{ion} &= \frac{q_i q_j}{r_{ij}} \\
b_{ij} &= \left(1+\zeta_{ij}^{\eta}\right)^{-\delta} \\
\zeta_{ij} &= \sum_{k\neq i,j} f_c(r_{ik})\left\{c + d\left(h - cos\theta_{ijk}\right)^2\right\} \\
&\times \exp\left[\alpha\left\{\left(r_{ij}-R_{ij}^e\right)-\left(r_{ik}-R_{ik}^e\right)\right\}^{\beta}\right] \\
f_c(r_{ij}) &= \begin{cases} 1 & r_{ij} \le R_1 \\ \frac{1}{2}\left[1+cos\left(\frac{\pi(r_{ij}-R_1)}{R_2-R_1}\right)\right] & R_1 < r_{ij} < R_2 \\ 0 & r_{ij} \ge R_2 \end{cases} \\
f_q(q_i) &= \frac{N_i(q_i)\left(N_i^0 - N_i(q_i)\right)}{N_i(0)\left(N_i^0 - N_i(0)\right)} \\
N_i(q_i) &= N_i^{neutral} - q_i
\end{aligned}
$$

[1] A. K. Rappé and W. A. Goddard III, J. Phys. Chem. 95, 3358 (1991).

[2] T. Kumagai, S. Izumi. S. Hara, S. Sakai, ICCM 2004, Singapore, 2004, Conference Digest pp. 75.

Potential fitting for thermal-oxidation growth process of Si

Potential fitted to crystal data

Variety of metastable and unstable structures containing 20-50 atoms are generated by classical MD.
amorphous, liquid, excess Si, O , SiO, O_2 in SiO_2, surface, interface

First-principles calc.
cohesive energy, force, charge

Improvement of the potential
minimize the mean square weighted deviation by genetic algorithm

Evaluation

Optimizing 111 parameters with more than 5100 structures and more than 800000 values obtained from the first-principles calculations

Overview of the fitting method

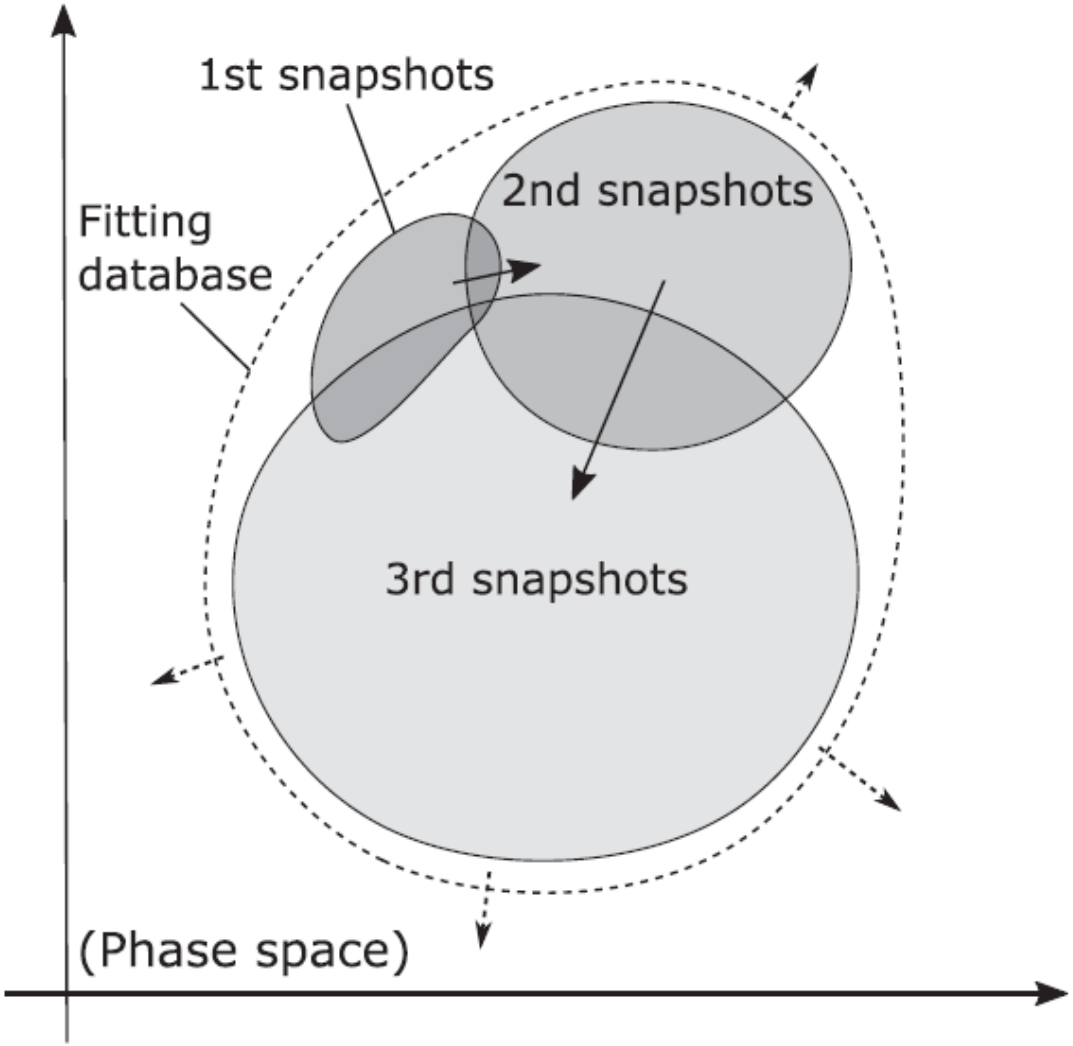

S. Takamoto, T. Kumagai, T. Yamasaki, T. Ohno, C. Kaneta, A. Hatano, and S. Izumi J. of Appl. Phys. **120**, 165109 (2016).

Energy comparison between Ab initio calculation and interatomic potentials

Energy

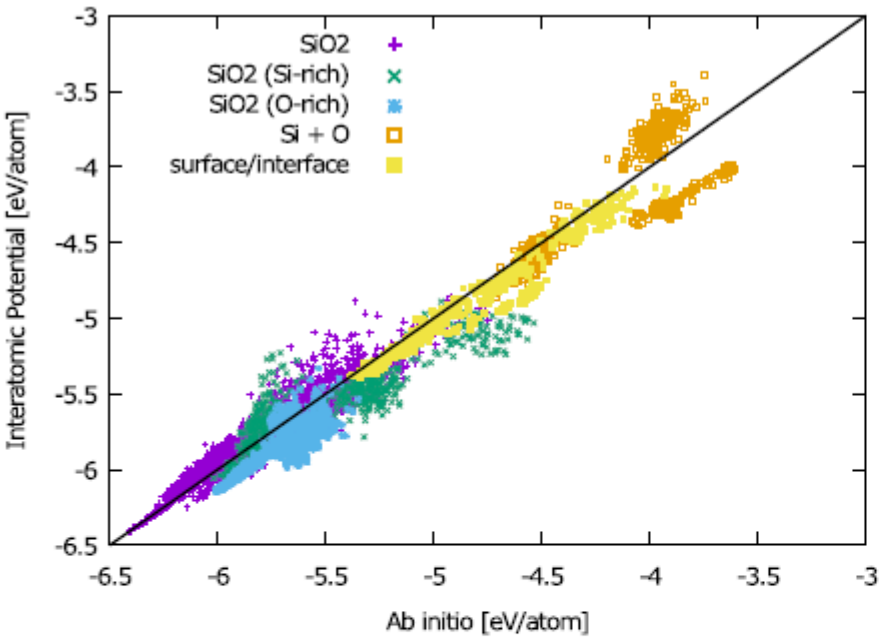

(a) Our interatomic potential

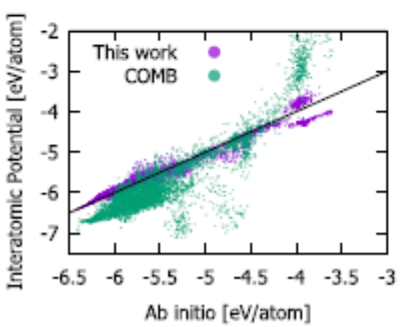

(b) COMB potential

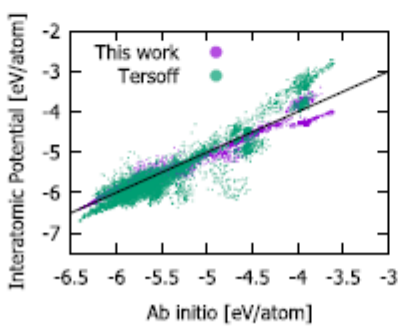

(c) Munetoh Tersoff-type potential

Force

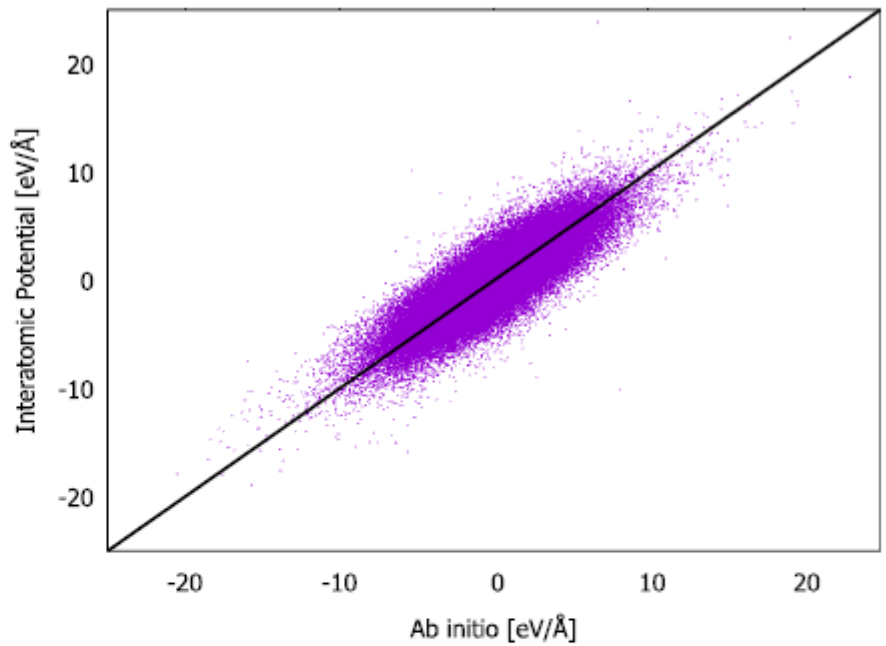

(a) Our interatomic potential

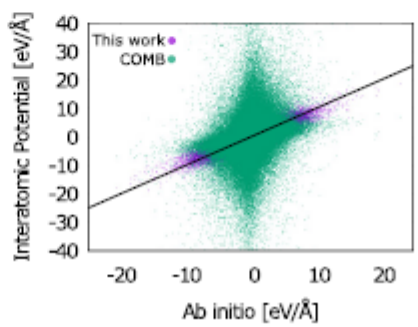

(b) COMB potential

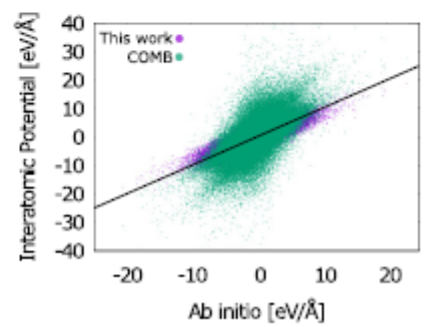

(c) Munetoh Tersoff-type potential

S. Takamoto, T. Kumagai, T. Yamasaki, T. Ohno, C. Kaneta, A. Hatano, and S. Izumi J. of Appl. Phys. **120**, 165109 (2016).

Radial Distribution Function

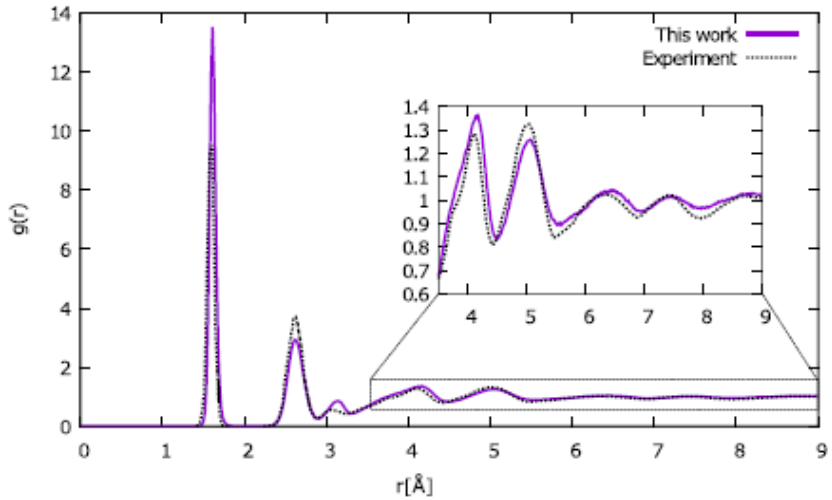

FIG. 6. RDF for amorphous SiO_2. Dotted line: neutron scattering.[46]

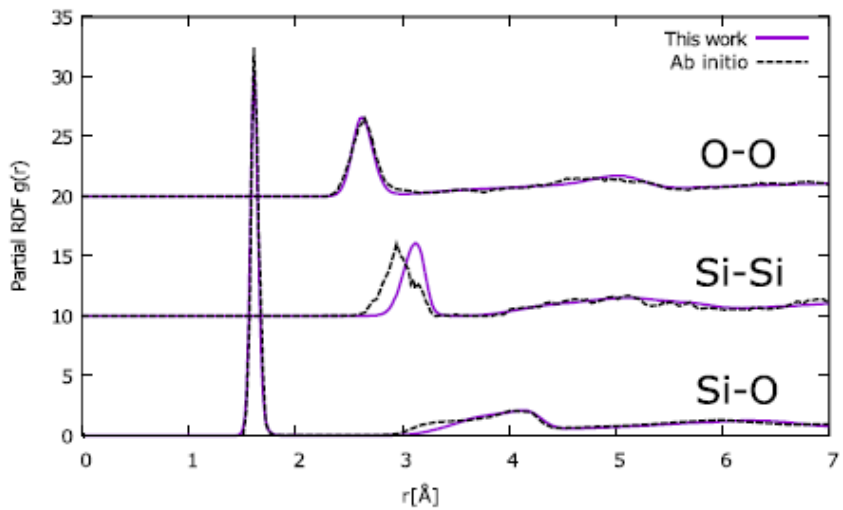

FIG. 7. Partial RDF for amorphous SiO_2. Dashed line: *ab initio*.[45]

S. Takamoto, T. Kumagai, T. Yamasaki, T. Ohno, C. Kaneta, A. Hatano, and S. Izumi J. of Appl. Phys. **120**, 165109 (2016).

Oxidation of Si(100) at 1200K

0 ns

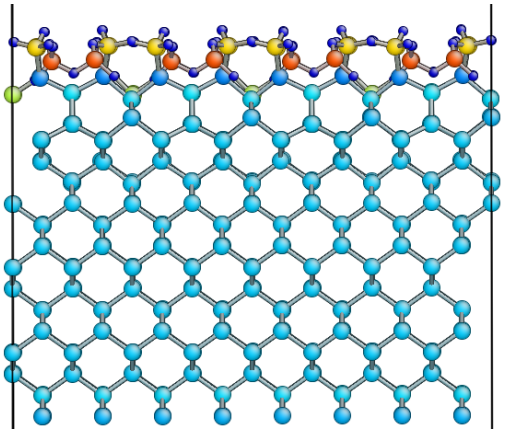

1312 atoms/cell

- 0-3.7 ns

動画

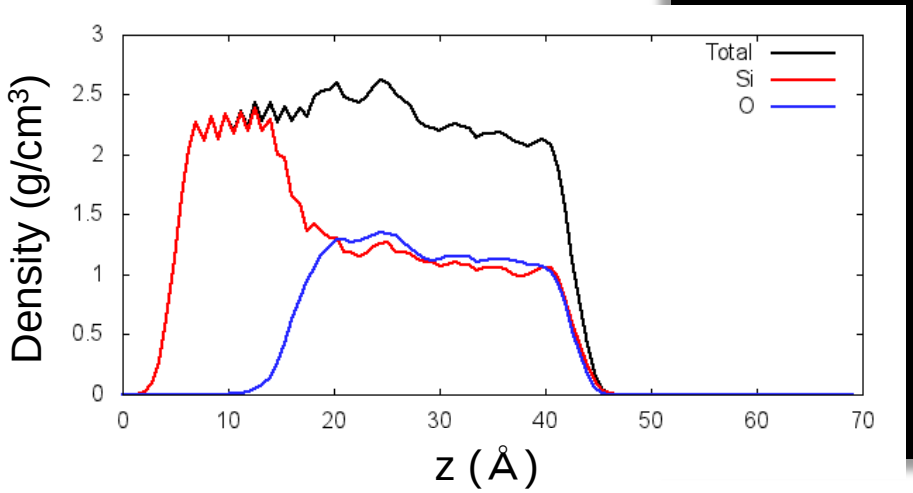

S. Takamoto, T. Kumagai, T. Yamasaki, T. Ohno, C. Kaneta, A. Hatano, and S. Izumi J. of Appl. Phys. **120**, 165109 (2016).

薄い酸化膜の電子スペクトル

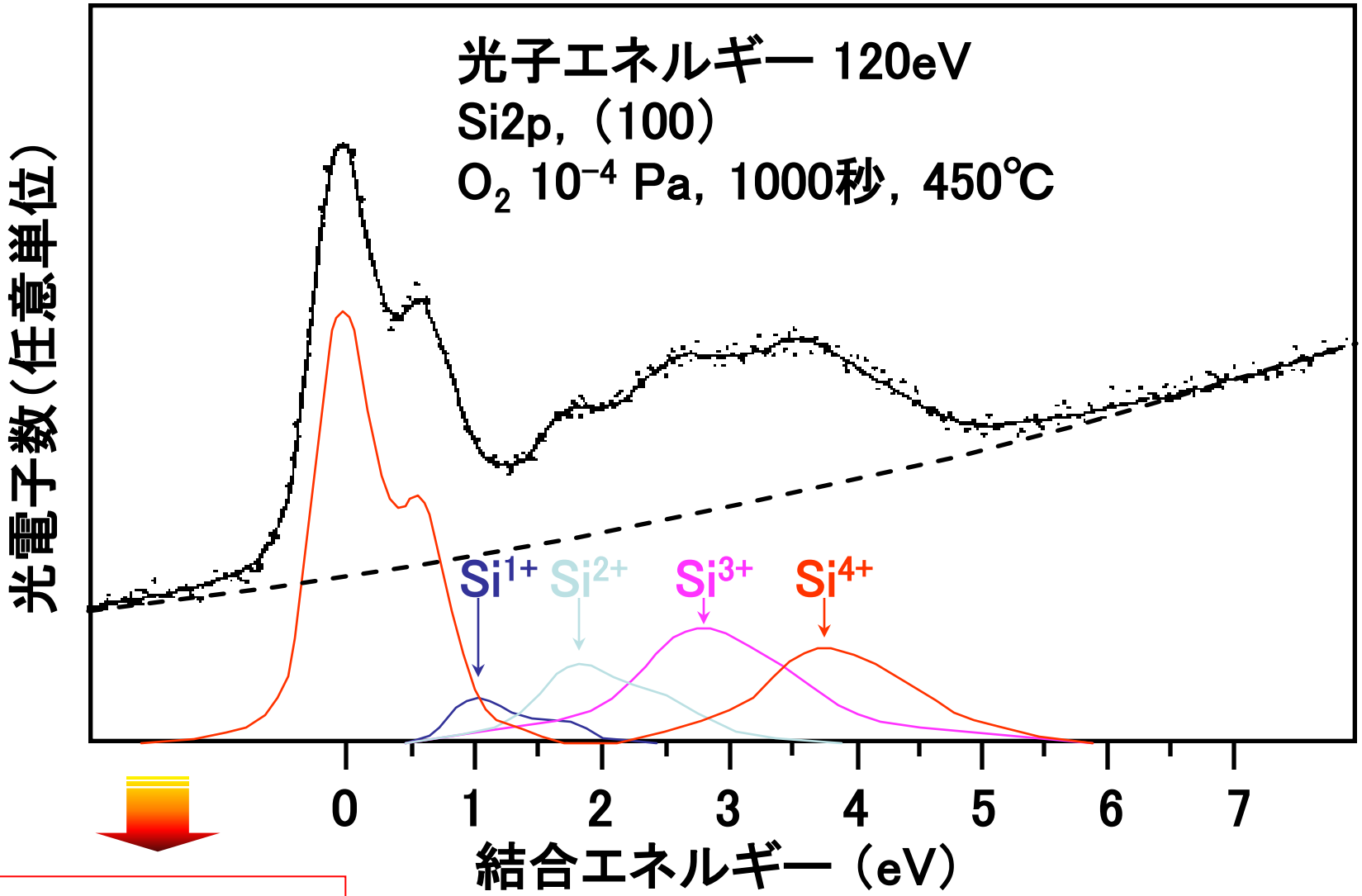

界面遷移層

Braun et al., Surt. Sci. 180, 279(1987).

Charge distribution at the Si/SiO_2 interface

1312 atoms/cell
1200K
NTV ensemble

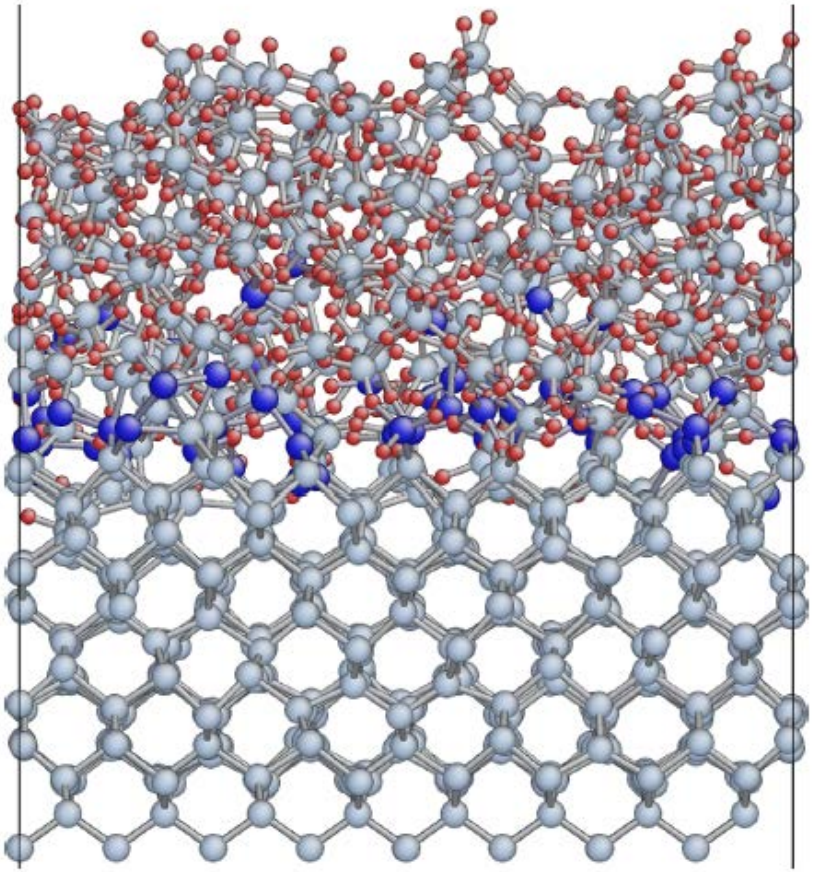

FIG. 12. Si/SiO_2 interface structure obtained by oxidation simulation. Larger spheres are Si atoms, smaller ones are O atoms. Blue atoms denote the 13th layer of crystal silicon.

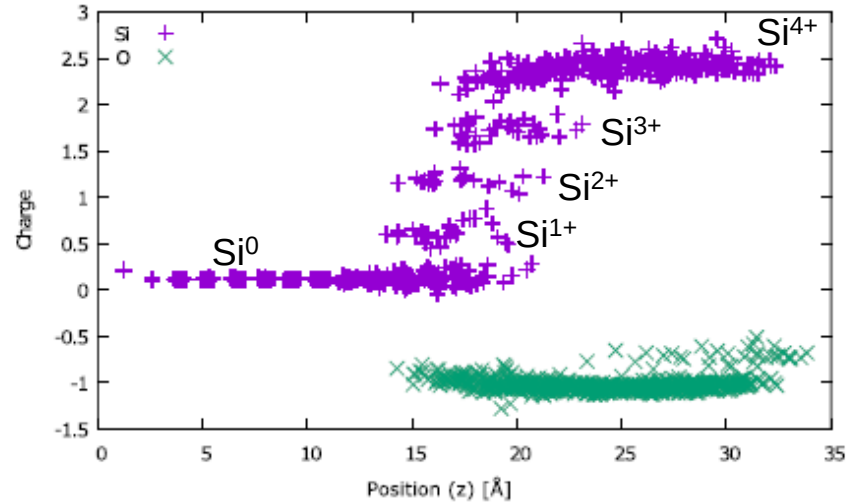

FIG. 13. Charge distribution along the z-axis for the Si/SiO_2 interface obtained by oxidation simulation.

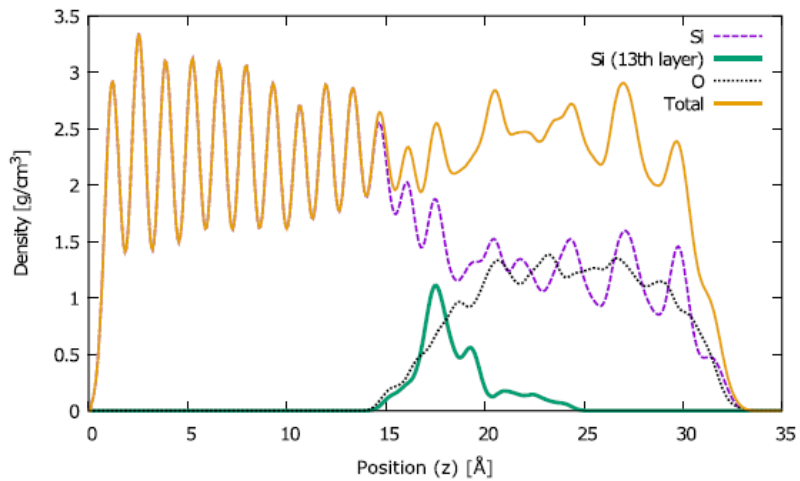

FIG. 14. Density distribution along the z-axis for Si/SiO_2 interface obtained by oxidation simulation. Smoothed by Gaussian distribution ($\sigma = 0.38$ Å).

S. Takamoto, T. Kumagai, T. Yamasaki, T. Ohno, C. Kaneta, A. Hatano, and S. Izumi J. of Appl. Phys. **120**, 165109 (2016).

Oxidation of SiC/SiO_2 interface structure

O(red)

Si(white)

C(gray)

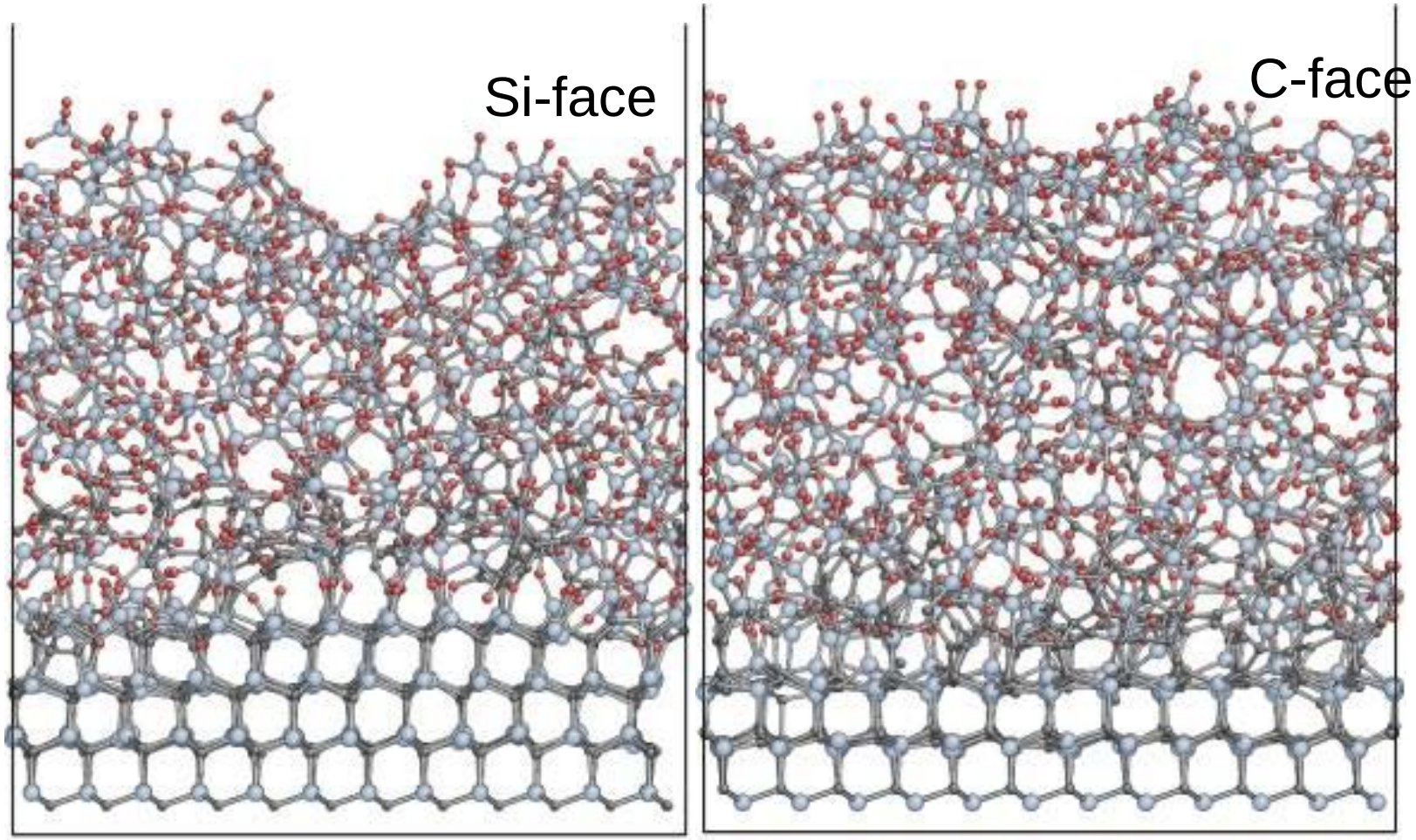

Takamoto et al. Jpn. Soc. Appl. Phys. Spring Meeting 2017

Distribution of suboxide of the Si-face interfac

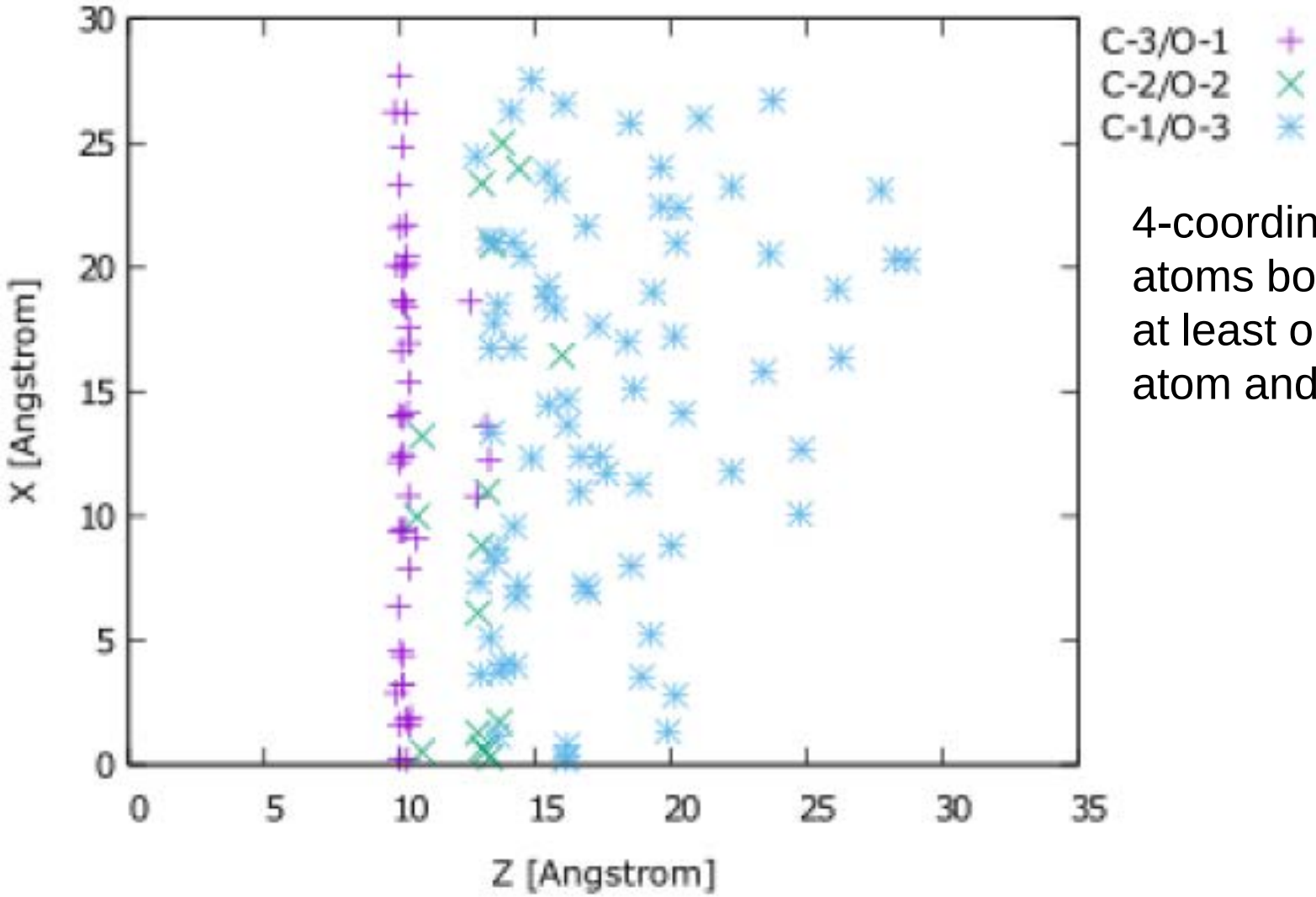

4-coordinated Si atoms bonded to at least one C atom and O atom

S. Takamoto, T. Kumagai, T. Yamasaki, T. Ohno, C. Kaneta, A. Hatano, and S. Izumi J. of Appl. Phys. **120**, 165109 (2016).

Calculation method for lattice thermal conductivity

Perturbed molecular dynamics

[1] M. Yoshiya et al., Mol. Simulat., **30**, 953 (2004).

[2] K. K. Mandadapu et al., J. Chem. Phys., **130**, 204106 (2009).

Equations of motion for atom *i*:

$$\begin{cases} \dot{\boldsymbol{r}}_i = \dfrac{\boldsymbol{p}_i}{m_i} & (1) \\ \dot{\boldsymbol{p}}_i = \boldsymbol{F}_i + \boldsymbol{D}_i \cdot \boldsymbol{F}_{\mathrm{ext}} & (2) \end{cases}$$

perturbation term

perturbation tensor

$\boldsymbol{r}_i$: position of atom i

$\boldsymbol{p}_i$: momentum of atom i

m_i : mass of atom i

$\boldsymbol{F}_i$: force exerted on atom i

Thermal conductivity κ :

$$\boxed{\kappa = \frac{V}{F_{\mathrm{ext}} T} \cdot \frac{1}{N} \sum_{s=1}^{N} J_x(s)} \qquad (3)$$

V : volume of the system

T : temperature

F_{ext} : magnitude of the perturbation

$J_x(s)$: instantaneous microscopic energy flux at step s

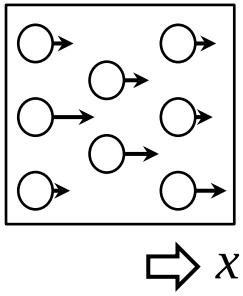

Tersoff type interatomic potentials[3]

Potential function $$\Phi = \sum_i \sum_{j>i} f_c\left[a_{ij} E_r\left(r_{ij}\right) - b_{ij} E_a\left(r_{ij}\right)\right]$$

Two-body terms
$$\begin{cases} E_r\left(r_{ij}\right) = A_{ij} \exp(-\lambda_{ij} r_{ij}) \\ E_a\left(r_{ij}\right) = B_{ij} \exp(-\mu_{ij} r_{ij}) \end{cases}$$

Three-body terms
$$\begin{cases} a_{ij} = \varepsilon_{ij} \left(1 + \beta_i^{n_i} \tau_{ij}^{n_i}\right)^{-\frac{1}{2n_i}} \\ b_{ij} = \chi_{ij} \left(1 + \beta_i^{n_i} \xi_{ij}^{n_i}\right)^{-\frac{m_i}{2n_i}} \\ \tau_{ij} = \sum_{k \neq i,j} f_c(r_{ik}) \delta_{ik} g(\theta_{ijk}) \\ \xi_{ij} = \sum_{k \neq i,j} f_c(r_{ik}) \omega_{ik} g(\theta_{ijk}) \exp\left[\sigma_{ik}\left(r_{ij} - r_{ik}\right)\right] \\ g\left(\theta_{ijk}\right) = 1 + \dfrac{c_i^2}{d_i^2} - \dfrac{c_i^2}{d_i^2 + (h_i - \cos\theta_{ijk})^2} \\ f_c\left(r_{ij}\right) = \begin{cases} 1 & (r_{ij} < R_{ij}) \\ \dfrac{1}{2}\left[1 + \cos\left(\pi \dfrac{r_{ij} - R_{ij}}{S_{ij} - R_{ij}}\right)\right] & (R_{ij} \leq r_{ij} < S_{ij}) \\ 0 & (S_{ij} \leq r_{ij}) \end{cases} \end{cases}$$

[3] J. Tersoff, Phys. Rev. B **37**, 6991 (1988);
J. Tersoff, Phys. Rev. B **38**, 9902 (1988).

Thermal conductivities of Si and Ge

@T = 1000 K

	This work	Exp. (W/mK)
Si	65	30～50[4-6]
Ge	24	17[6,7]

[4] W. S. Capinski et al., Appl. Phys. Lett. **71**, 2109 (1997).
[5] M. Kazan et al., J. Appl. Phys. **107**, 083503 (2010).
[6] C. J. Glassbrenner et al., Phys. Rev. **134**, A1058 (1964).
[7] M. G. Holland, Phys. Rev. **132**, 2461 (1963).

Phonon mode analysis

Structural relaxation Tersoff type three-body potential [2]	LAMMPS [1]
↓	
Generation of small displacement of each atom	Phonopy [3]
↓	
Calculation of force on each atom	LAMMPS
↓	
Dynamical Matrix Phonon mode analysis within the harmonic approximation VDOS, Participation Ratio	Phonopy

[1] S. Plimpton, J. Comp. Phys., **117**, 1 (1995) ; http://lammps.sandia.gov/.

[2] J. Tersoff, Phys. Rev. B **37**, 6991 (1988) ; J. Tersoff, Phys. Rev. B **38**, 9902 (1988).

[3] A. Togo and I. Tanaka, Scr. Mater., **108**, 1 (2015) ; http://atztogo.github.io/phonopy/.

Model structures of Si/Ge superlattice and SiGe alloy

Si/Ge superlattice

SiGe alloy

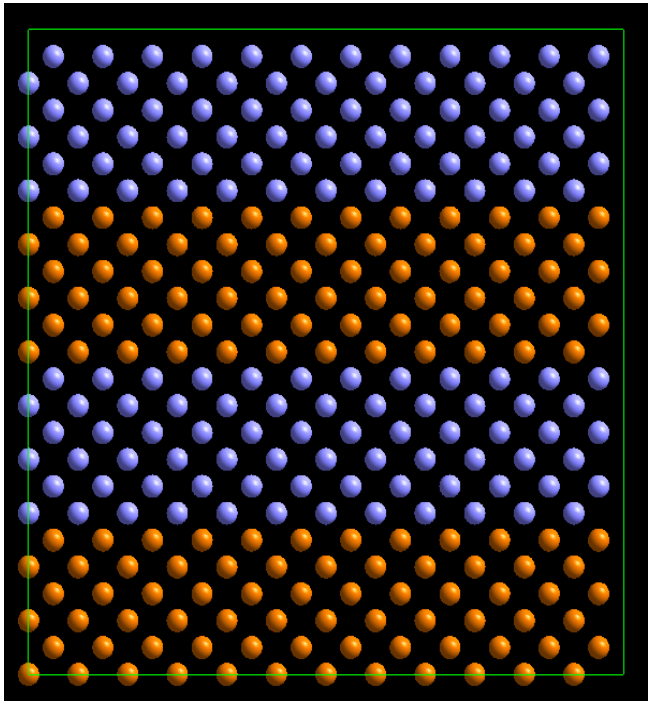

1728 atoms/cell

Si

Ge

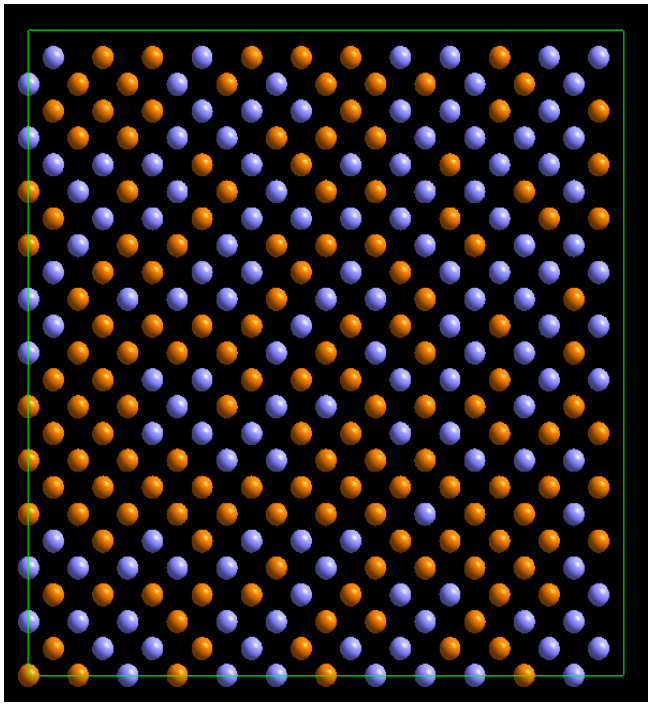

Vibrational DOS of Si and Ge crystals

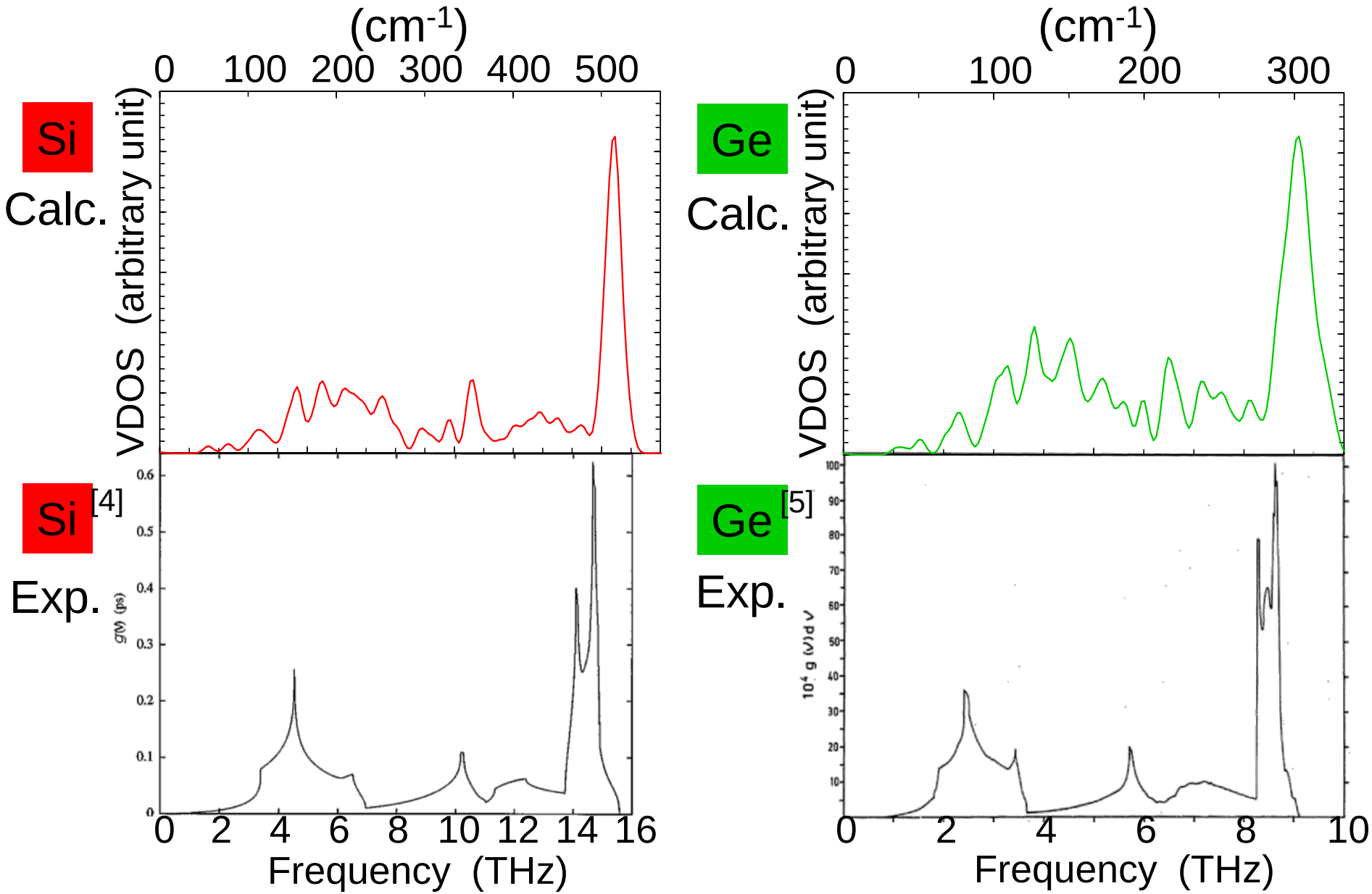

[4] C. Flensburg et al., Phys. Rev. B **60**, 284 (1999).

[5] G. Nilsson et al., Phys. Rev. B **6**, 3777 (1972).

Vibrational DOS of SiGe alloy and Si/Ge siperlattice

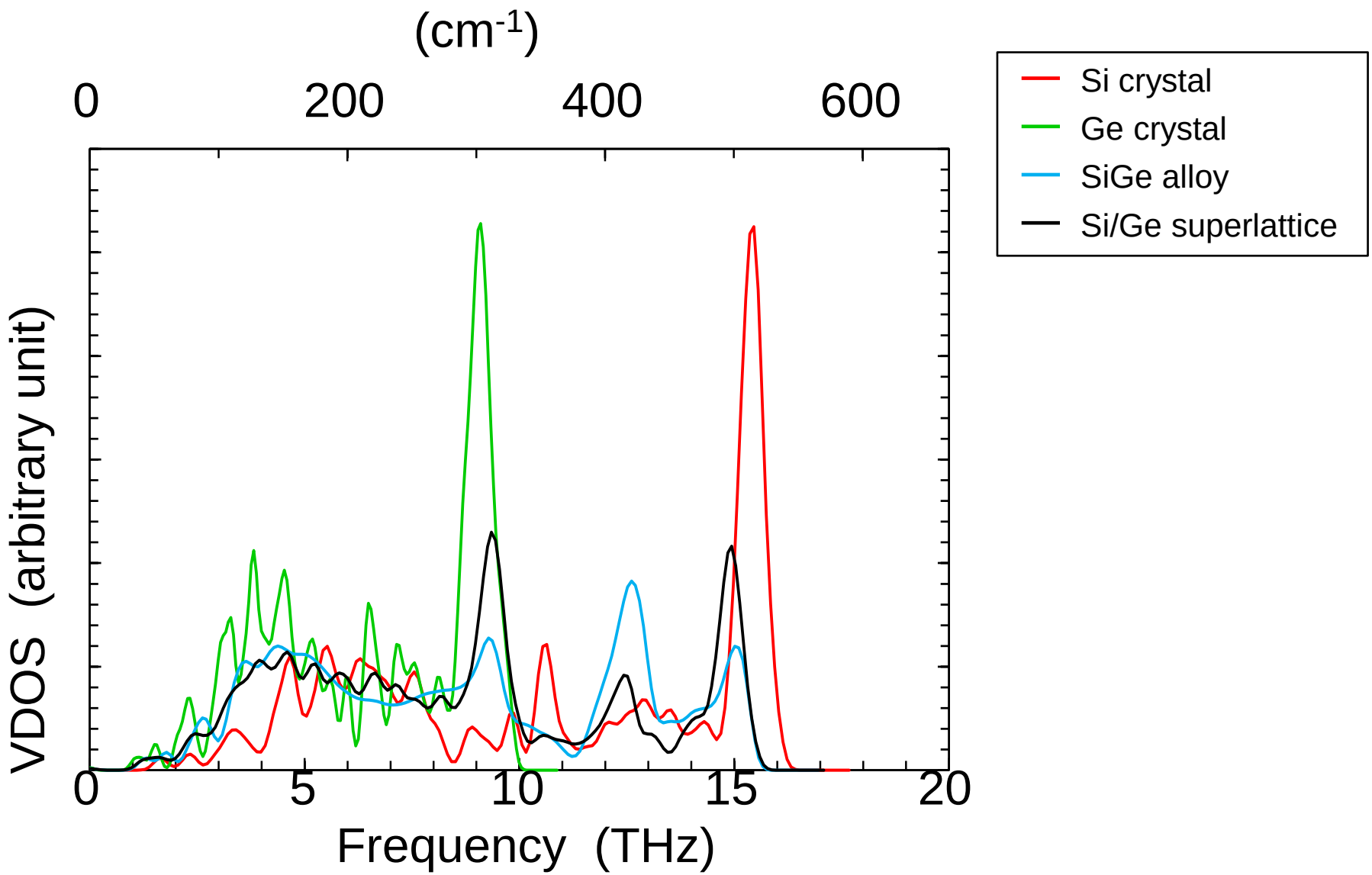

N. Takahashi and C. Kaneta,
The Japan Soc. of Appl. Phys. autumn meeting 2016

Participation Ratio

<u>Participation ratio</u> [6]

characterizes the mode localization.

[6] A. Bodapati, P. K. Schelling, S. R. Phillpot, and P. Keblinski, Phys. Rev. B **74**, 245207 (2006).

$$p_\lambda^{-1} = N \sum_i \left(\sum_\alpha e^*_{i\alpha,\,\lambda}\, e_{i\alpha,\,\lambda} \right)^2$$

N : number of atoms in unit cell

$e_{i\alpha,\,\lambda}$: vibrational eigenvector component α (*x,y,or z*) of i atom in mode λ

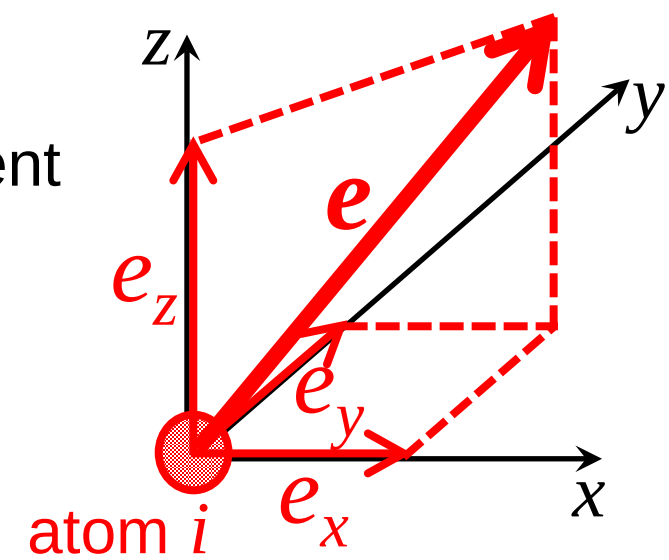

$p_\lambda \sim O(1/N)$ for localized modes

$O(1)$ for delocalized modes

Participation ratio and thermal conductivity

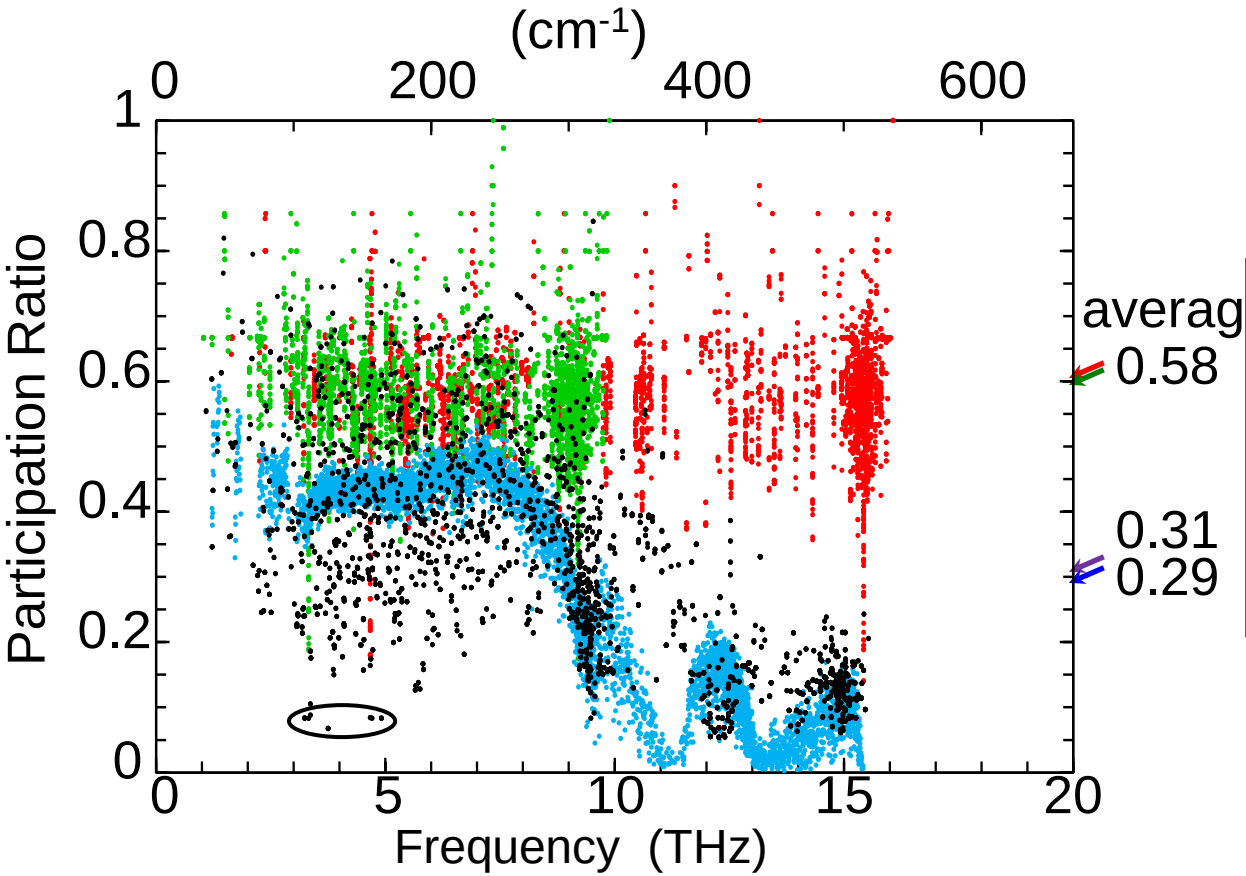

Termal conductivity
Calculated at 1000 K
(W/mK)

Si crystal	65
Ge crystal	24
SiGe alloy	1.07
Si/Ge	0.94

N. Takahashi and C. Kaneta,
The Japan Soc. of Appl. Phys. autumn meeting 2016

Application of phonon mode analysis and genetic algorithm to design Si/Ge structure with low thermal conductivity

High throughput evaluation using **GA**

Si/Ge superlattice structure

Phonon mode analysis

Thermal conductivity κ

Inverse design

Correlation between κ and Participation ratios

Descriptor

In this work,

we analyzed about 350000 structures.

The probability to find 10 best candidates:

1) more than 99% by searching for 43% of all structures (about 50 generations)
2) more than 90% by searching for 22.7% of all structures

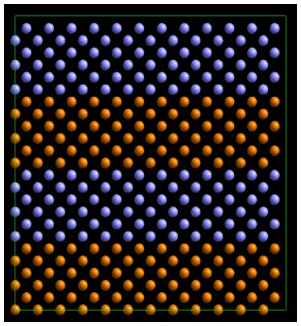

Si

Ge

Atomistic simulations in Industry

for example…

Applications \ methods	ab initio calc.	Tight Binding	Classical MD	Monte Carlo	Phenomenological calc.	Experiments
nano CMOS	○	○	○	○	○	○
Power devices	○	○	○	○		○
Fuel cells	○		○			○
Solar cells	○	○			○	○
etc.	○	○	○	○	○	○

Academia (Science)

Physics, Chemistry, and Methodology

Industry (Technology)

Optimum solution within a limited period and budget

Future of atomistic simulations

Role of simulation

Understanding
Tools for Modeling
etc.

Parameter search:
Composition, growth temperature …

Evaluation

Design:
materials, devices, and the recipes etc.

Discovery

Atomistic simulation as a technology

quality: appropriate accuracy and cost for calculation

High performance quantum simulation

Parametrization based on the first principles calc.

Multiscale, multiphysics simulations

Process parameter survey
Materials informatics

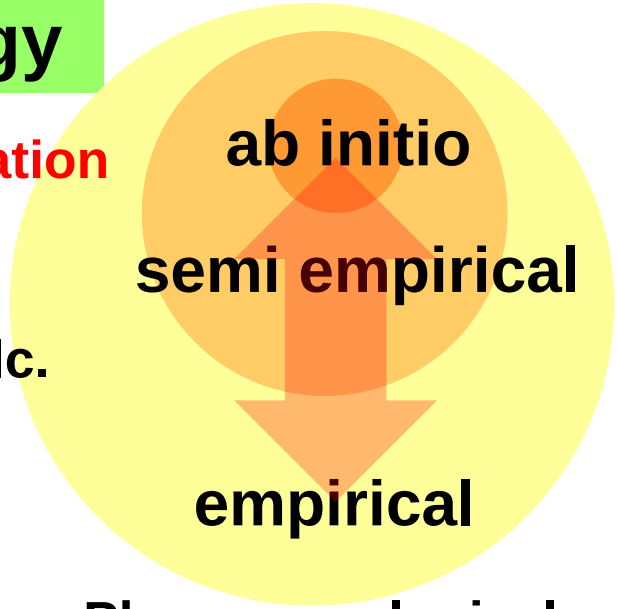

Phenomenological
(modeling, equations)